Two Dimensional Turbulence in the Atmosphere and Oceans

Robert Horton

August 19, 2005

Abstract

This dissertation is concerned with the evolution of turbulent flow in the atmosphere and oceans. The properties of turbulence on an f-plane, on a beta-plane and over shallow orography are discussed and the results of decaying turbulence models presented. Attention is given in particular to the evolution of the energy and enstrophy spectra.

For the f-plane case it is shown that energy is transfered from small to large scales whilst enstrophy is transfered from large to small scales. The flow is initialised as a thin wavenumber distribution of vorticity. As the flow evolves, thin streamers of vorticity are formed after which the flow becomes organised into a number of vortices. These are advected by the base flow but rarely interact. The energy spectra produced are somewhat steeper than the k^{-3} shape predicted by Kraichnan.

The addition of differential planetary vorticity complicates the situation by the addition of Rossby waves. It is shown that for length scales above a threshold the flow is dominated by Rossby waves whereas for length scales below this threshold the flow is dominated by turbulence. The anisotropy of Rossby waves means that the wave-turbulence boundary is not isotropic. The tendency for the turbulence to become concentrated at the lowest available wavenumber leads to the turbulent part of the flow also becoming anisotropic.

It is shown that placing orography in an f-plane flow causes a patch of negative vorticity to form above the orography but does not otherwise have a large effect on the evolution of the flow. The addition of orography to flow on a beta-plane, however leads to the initialisation of Rossby waves.

Declaration

I confirm that this is my own work, and the use of all material from other sources has been properly and fully acknowledged.

Robert Horton

Acknowledgements

This work was funded by an advanced training studentship from the Natural Environment Research Council, award number NER/S/M/2004/12618.

I would like to thank my supervisor, Dr Maarten Ambaum, for all his help and support. I would also like to thank Dr David Stephenson and Prof. Peter Rhines who both provided a number of helpful suggestions.

Finally I would like to thank the rest of the MSc course for making the year enjoyable, my family for their continual support and Sally for proofreading the draft and for generally being there.

Robert Horton
August 2005

Contents

Chapter 1

Introduction

This work is concerned with the evolution of turbulent flow in the atmosphere and oceans. Turbulence refers to "the chaotic, nonlinear motion of fluids that are near to a state of geostrophic and hydrostatic balance"[20]. Particular attention is paid to the evolution of the energy and enstrophy spectra for such flows. We shall consider initially flow on an f-plane then extend this to a beta-plane. Finally we shall look at the effect of shallow orography on turbulence.

1.1 History

The first attempts to explain the large scale dynamics of the atmosphere [9] date from the seventeenth century. In 1687 Halley proposed that the trade winds were caused by the differential heating of different lattitudes. Hadley went slightly further, in 1720 proposing that the surface trade winds must be balanced by poleward flow at higher altitude.

The latter part of the eighteenth century saw the start of attempts to express the dynamics of fluid motion mathematically. The equations of motion and continuity equation for an ideal fluid [1] were first derived by Euler. Coriolis realised the importance of the Earth's rotation and derived an equation set from an inertial frame of reference.

1.1.1 Two dimensional flow

In the first half of the twentieth century much work on geophysical fluid dynamics was produced by Taylor. One of Taylor's most important results is the Taylor-Proudman theorem. Consider the Euler momentum equation for a fluid rotating with angular velocity $\boldsymbol{\Omega}$.

$$\frac{\mathrm{D}\boldsymbol{u}}{\mathrm{D}t} = -2\boldsymbol{\Omega} \times \boldsymbol{u} - \boldsymbol{g}_e - \frac{1}{\rho} \bigtriangledown p$$

where $\boldsymbol{u}$ is the velocity vector, $\boldsymbol{g}_e$ the effective gravitational field strength (i.e. gravitational field plus centrifugal force), ρ is density and p pressure. If we assume the flow is slow moving (so the acceleration term may be neglected) and incompressible this can be rewritten as

$$2\boldsymbol{\Omega} \times \boldsymbol{u} + \boldsymbol{g}_e + \bigtriangledown \left(\frac{p}{\rho} \right) = 0$$

Taking the curl of this gives

$$(\boldsymbol{\Omega}.\bigtriangledown)\, \boldsymbol{u} + \boldsymbol{\Omega}\, (\bigtriangledown.\boldsymbol{u}) = 0$$

Since the flow is incompressible $\bigtriangledown.\boldsymbol{u} = 0$ so

$$(\boldsymbol{\Omega}.\bigtriangledown)\, \boldsymbol{u} = 0$$

So $\boldsymbol{u}$ cannot vary in the direction parallel to the rotation axis. This means that a rotating fluid will only move in the direction perpendicular to the axis of rotation.

This result is mainly relevant for laboratory rotating tank experiments. In the atmosphere and oceans the constraint resulting from stratification results in an approximately two dimensional flow.

Taylor further showed that in such a system the absolute vorticity, ζ of fluid elements is conserved, i.e.

$$\frac{\mathrm{D}\zeta}{\mathrm{D}t} = 0$$

For the case that the flow is subject to forcing and dissipation this can be extended to

$$\frac{\mathrm{D}\zeta}{\mathrm{D}t} = \text{forcing} - \text{dissipation} \tag{1.1}$$

Taylor also showed that for a three dimensional turbulent flow energy is cascaded from macroscopic to microscopic scales, via vortex stretching, and demonstrated the impossibility of this for two dimensional flows. The forward cascade of enstrophy and inverse cascade for energy were initially envisaged by Richardson and formalised by Kolmogorov and Oboukhov. Kolmogorov derived[10] the $k^{-5/3}$ law for the form of the energy spectrum for three dimensional turbulence which also applies to two dimensional turbulence for the part of the spectrum dominated by energy transfer. Kraichnan extended this to give the k^{-3} law[11] for the part of the spectrum dominated by enstrophy transfer.

Interest in two dimensional turbulence arose initially for use in early computational fluid dynamics experiments. One of the earliest to specifically investigate turbulence was Lilly[12], who in 1969 used a numerical simulation of the two dimensional incompressible Navier-Stokes equations to investigate numerically the character of two dimensional turbulence. Improvements in computing power meant that three dimentional experiments became practical.

McWilliams produced a series of high resolution simulations[17, 16] of two dimensional turbulence. In particular these (and most subsequent studies) produced an energy spectrum much steeper than that predicted by Kraichnan, it is argued that this is due to the effect of dissipation, this is despite the use of hyperviscosity, $-\bigtriangledown^4\xi$, (as opposed to Newtonian viscosity, $-\bigtriangledown^2\xi$),where ξ is relative vorticity such that $\zeta = \xi + f$, to represent the dissipation term in (1.1). This is to attempt to limit the action of diffusion to the smallest scales. McWilliams observes that the turbulent flow becomes organised into a number of symmetric eddies which have a long lifetime compared to the eddy turnover time and which are advected by the flow within the domain and rarely interact. This effectively limits the inverse energy cascade.

Although much of the early interest in two dimensional turbulence was due to uses in early numerical experiments, interest has remained despite the increase in computing power making three dimensional simulations practical. The assumptions behind two dimensional turbulence theories, namely a homogeneous fluid rotating rapidly (relative to the flow), apply approximately to the atmosphere and oceans, at least at large scales. Clearly there are severe limitations to this approximation; baroclinic effects play an important role in weather system development, at small scales in the atmosphere in particular three dimensional effects such as convection are important and at larger scales differential planetary vorticity has an important effect in the form of Rossby waves. Nonetheless we would expect effects of two dimensional turbulence to be visible in the atmosphere and oceans and it is an important starting point for understanding the characteristics of geostrophic turbulence.

The enstrophy cascade relies on the stretching of (potential) vorticity contours. Other effects in the atmosphere and oceans, such as differential rotation, stratification and orography may limit the stretching of these contours. This is discussed by Rhines[20].

1.1.2 The Rossby Wave

During the Second World War [6], Carl-Gustaf Rossby wrote a series of papers [24, 22, 23] which attempted to describe large scale atmospheric motions using a wave equation, later known as Rossby waves. This wave behaviour results from the differential planetary vorticity with respect to latitude (the "beta effect"). The use of a wave equation meant that the evolution could be predicted simply and was thus highly significant.

Following the Second World War it was observed that things were actually somewhat more complex than permitted by Rossby's wave equation. In particular, it was observed that atmospheric motions are at least to some extent turbulent. Interest therefore turned towards the use of finite difference methods [5, 21] to solve nonlinear partial differential equations describing atmospheric motions.

Rossby waves by no means provide a complete explanation for atmospheric motions but nonetheless many of the features predicted by Rossby are clearly evident in the large scale dynamics of the mid to upper troposphere for time scales large compared to a day. The Rossby wave remains an important dynamical feature for understanding atmospheric dynamics. Rhines[19] describes the transition from wave-like to turbulent dynamics and provides a boundary wavelength. For length scales smaller than this turbulent behaviour will dominate whereas for larger scales Rossby waves will be dominant. Rhines also observes that the anisotropy of Rossby waves means that this boundary is not isotropic. This is extended by Vallis and Maltrud[13, 26] to provide an expression for the anisotropic wave turbulence boundary. The tendency for the turbulent element to transfer to the smallest wavenumber available means that the turbulence is therefore no longer isotropic.

1.1.3 Other factors affecting turbulent evolution

The presence of uneven topography can have a significant effect on both atmospheric and oceanic dynamics. In the atmosphere the major mountain ranges such as the Himalaya and Rockies can both lead to the generation of weather systems. The effect of topography on vorticity evolution was originally shown by Taylor. Charney and Elliasen[4] showed that orography can be important in initiating Rossby waves in the atmosphere (this is also discussed by Holton[8]).

The main factor not discussed here is that of stratification in the atmosphere. Charney[2] first derived the theoretical framework for stratified geostrophic turbulence (See also [3]). McWilliams[14, 15] produced a series of high resolution simulations of forced and decaying stratified geostrophic turbulence.

1.2 Potential Vorticity

We have seen that for rotating flow the vorticity of fluid elements is conserved. This may be extended to systems where this is not the case by defining potential vorticity, q, which, in the absence of forcing or dissipation, is conserved, such that

$$\frac{\mathrm{D}q}{\mathrm{D}t} = 0 \tag{1.2}$$

The form of q depends on the model equations used. The simplest case is for two dimensional flow, $q = \xi$. This is a concept we shall be making extensive use of in the following chapters.

Chapter 2

Two Dimensional Turbulence

2.1 Properties of two dimensional turbulence

We shall consider initially the characteristics of turbulent flow in a two dimensional, inviscid fluid. We have already seen that the absolute vorticity, ζ, of elements in such a fluid is conserved. Since the Coriolis parameter, f, is constant it follows that the relative vorticity, ξ is conserved such that

$$\frac{D\xi}{Dt} = 0 \tag{2.1}$$

Considering a rectangular domain with no slip boundary conditions, vorticity may be expressed as a Fourier spectrum

$$\xi(\boldsymbol{x}) = \iint \hat{\xi}(\boldsymbol{k}) e^{i\boldsymbol{k}.\boldsymbol{x}} \mathrm{d}k_x \mathrm{d}k_y \tag{2.2}$$

where $\boldsymbol{x} = (x, y)$ is a position vector, $\boldsymbol{k} = (k_x, k_y)$ is a wave vector.

The enstrophy per unit volume of a domain D is defined as

$$Z = \frac{1}{2D} \int_D \xi^2 dD$$

This may be expressed as a Fourier series

$$Z = \frac{1}{2} \iint_D |\hat{\xi}(\boldsymbol{k})|^2 \mathrm{d}k_x \mathrm{d}k_y \tag{2.3}$$

The kinetic energy per unit mass of the domain is given by

$$E = \frac{1}{2D} \int_D \boldsymbol{u}.\boldsymbol{u} dD$$

As with vorticity this may be expressed in terms of Fourier components

$$E = \frac{1}{2} \iint |\hat{\boldsymbol{u}}(\boldsymbol{k})|^2 \mathrm{d}k_x \mathrm{d}k_y$$

Thus far we have considered vorticity and energy in terms of a wave vector, $\boldsymbol{k}$, with components k_x, k_y. We wish to be able to make calculations in terms of the wavenumber, k, where $k = |\boldsymbol{k}|$. Each wavenumber has a whole 'shell' of wavevectors with the corresponding wavenumber. We therefore define $Z(k)$ and $E(k)$ as the summation of all wavevectors with magnitude k of enstrophy and energy respectively. This may be expressed via polar integration as

$$Z(k) = \int_0^{2\pi} \left| \left\langle \hat{\xi}(\boldsymbol{k}) \right\rangle \right|^2 \mathrm{d}\theta \tag{2.4}$$

and

$$E(k) = \int_0^{2\pi} |\langle \hat{u}(\boldsymbol{k}) \rangle|^2 \, \mathrm{d}\theta \tag{2.5}$$

where the $\boldsymbol{k}$ subscript represents the wavevector with magnitude k and $\theta = \tan^{-1}(k_y/k_x)$ hence

$$Z(k) = \pi k \left| \left\langle \hat{\xi}(k) \right\rangle \right|^2$$

and

$$E(k) = \pi k \left| \langle \hat{\boldsymbol{u}}(k) \rangle \right|^2$$

where angle brackets denote an average in wavenumber space for magnitude k.

We may now derive a relationship between energy and enstrophy for a given wavenumber by making a substitution for stream function, ψ. For geostrophic flow

$$\begin{pmatrix} u \\ v \end{pmatrix} = \begin{pmatrix} -\frac{\partial \psi}{\partial y} \\ \frac{\partial \psi}{\partial x} \end{pmatrix}$$

which may be expressed in terms of Fourier components as

$$\begin{pmatrix} \hat{u}_{\boldsymbol{k}} \\ \hat{v}_{\boldsymbol{k}} \end{pmatrix} = \begin{pmatrix} -ik_y \hat{\psi}_{\boldsymbol{k}} \\ ik_x \hat{\psi}_{\boldsymbol{k}} \end{pmatrix}$$

We may therefore express energy in terms of streamfunction by

$$\langle \hat{\boldsymbol{u}}_{\boldsymbol{k}} . \hat{\boldsymbol{u}}_k^* \rangle = k^2 |\psi_k|^2$$

Vorticity may also be expressed in terms of streamfunction

$$\xi = \nabla^2 \psi$$

Expressed as Fourier components this gives

$$\begin{aligned} \hat{\xi}_{\boldsymbol{k}} &= -k_x^2 \hat{\psi}_k - k_y^2 \hat{\psi}_k \\ &= -k^2 \hat{\psi}_k \end{aligned}$$

hence

$$\hat{\xi}_{\boldsymbol{k}} \hat{\xi}_{\boldsymbol{k}}^* = k^4 |\hat{\psi}_{\boldsymbol{k}}|^2$$

therefore, energy and vorticity are related by

$$E(k) = k^2 Z(k)$$

2.1.1 Energy and Enstrophy Transfer

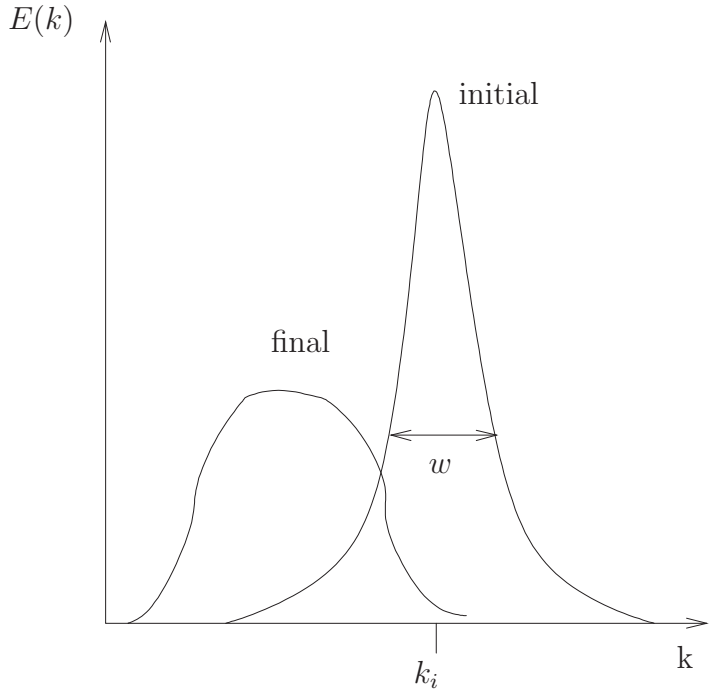

Figure 2.1: Anticipated change in energy distribution for a system initialised with a thin energy spectrum. The thin spectrum evolves into a wider spectrum, centred at a lower wavenumber. As the total energy is conserved, the height of the peak is reduced.

We now wish to consider how the distributions of energy and enstrophy will evolve with time. Consider a flow initialised such that energy is distributed amongst a narrow band of wavenumbers, (Figure 2.1). The first raw moment of $E(k)$ is given by

$$k_i = \frac{\int kE(k)dk}{\int E(k)dk} \tag{2.6}$$

which gives a measure of the central wavenumber of the energy spectrum.

The second moment of $E(k)$ taken around the mean, k_i gives a measure (variance) of the width of the energy spectrum.

$$w^2 = \int (k - k_i)^2 E(k)dk \tag{2.7}$$

In order to understand how k_i varies with time, we will take the time derivative of (2.7). We will make three assumptions about the evolution of the energy spectrum. Firstly we shall assume that the total energy in the system, $\int E(k)\mathrm{d}k$ remains constant. We shall assume that the system is scaled such that the total

energy is equal to unity. Secondly we assume that the width, w of the energy spectrum increases with time. This seems a reasonable assumption as one would expect energy in a narrow spectrum to be transfered to surrounding wavenumbers. Finally we assume that the enstrophy of the system, $\int k^2 E(k)$ is conserved. We have already established that, in the absence of forcing or dissipation, the vorticity of fluid elements is conserved, therefore the enstrophy is also conserved.

Expanding (2.7) gives

$$w^2 = \int k^2 E(k)\mathrm{d}k + k_i^2 \int E(k)\mathrm{d}k - 2k_i \int kE(k)\mathrm{d}k$$

substituting in (2.6) gives

$$w^2 = \int k^2 E(k)\mathrm{d}k - k_i^2 \int E(k)\mathrm{d}k$$

taking the time derivative of this gives

$$\frac{\mathrm{d}w^2}{\mathrm{d}t} = \frac{\mathrm{d}}{\mathrm{d}t}\int k^2 E(k)\mathrm{d}k - \frac{\mathrm{d}}{\mathrm{d}t}k_i^2 \int E(k)\mathrm{d}k$$

Assuming that energy and enstrophy are both conserved this gives

$$\frac{\mathrm{d}w^2}{\mathrm{d}t} = -\frac{\mathrm{d}k_i^2}{\mathrm{d}t}$$

If we assume that the width of the energy spectrum increases, i.e. w increases, this implies that as time progresses energy will shift from large wave number (small scale) to small wave number (large scale).

A similar argument shows that enstrophy is transferred from small to large wave number (i.e. large to small scale). The proof is most easily given by consideration of a length scale, q such that $q = 1/k$ as given by [25].

The first raw moment is given by

$$q_i = \frac{\int qZ(q)\mathrm{d}q}{\int Z(q)\mathrm{d}q} \tag{2.8}$$

The second moment, centred around the mean, q_i, is given by

$$w^2 = \int (q - q_i)^2 Z(q)\mathrm{d}q \tag{2.9}$$

Expanding (2.9) and substituting in (2.8) gives

$$w^2 = \int q^2 Z(q)\mathrm{d}q - q_i^2 \int Z(q)\mathrm{d}q$$

However $\int q^2 Z(q)\mathrm{d}q$ is the total energy, which we assume is conserved, as is $\int Z(q)\mathrm{d}q$ which is the total enstrophy. This gives

$$\frac{\mathrm{d}q_i^2}{\mathrm{d}t} = -\frac{\mathrm{d}w^2}{\mathrm{d}t} < 0$$

So, the length scale describing the mean enstrophy wavenumber is reduced, hence the wavenumber is increased.

2.1.2 Inertial Ranges

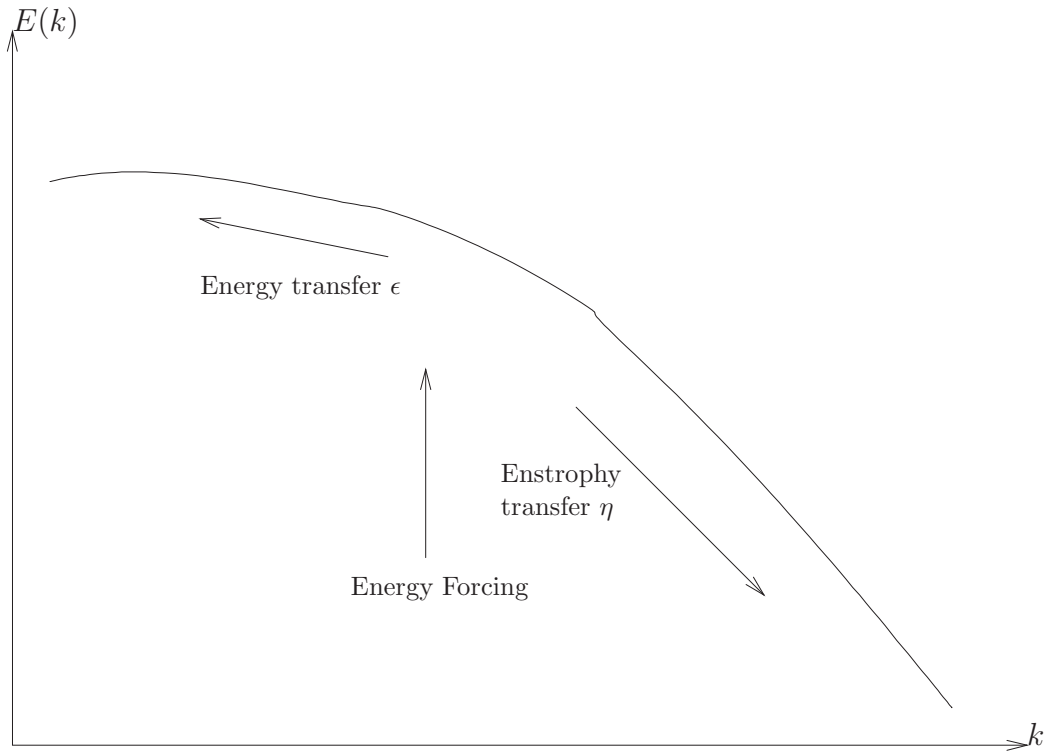

Figure 2.2: Idealised energy wavenumber distribution in two dimensional turbulence

We have shown that in a two dimensional turbulence system with energy forcing at some intermediate wavenumber, energy will be transfered toward small wavenumbers and enstrophy toward large wavenumbers (figure 2.2). We now wish determine the shape of the energy spectrum.

The idea of deriving a profile of energy with respect to wavenumber was first presented by Kolmogorov[10] and extended to two dimensional turbulence by Kraichnan[11]. The derivation presented here follows the form of that given by [25].

2.1.3 Inverse energy cascade region

We consider initially the part of the spectrum dominated by the transfer of energy from large to small wavenumbers. If energy is supplied to the system at rate ϵ and the system is in equilibrium then energy must also be transfered at rate ϵ. Kolmogorov assumes that the shape of the energy spectrum is determined only

by the energy flux and the wavenumber, i.e.

$$E(k) = f(\epsilon, k)$$

Scaling argument

The most straightforward method of determining the shape of $E(k)$ is through dimensional analysis, as given by[25].

$E(k)$ has dimensions of L^3/T^2, ϵ has dimensions of L^2/T^3 and k has dimensions of $1/L$.

In order to achieve the correct time dimensions we therefore require that

$$E(k) \sim \epsilon^{2/3} g(k)$$

Thus the only dimensionally correct solution is

$$E(k) = \kappa \epsilon^{2/3} k^{-5/3}$$

where κ is a constant of proportionality.

Eddy turnover time argument

A slightly more rigorous argument can be made by considering the eddy turnover time, $\tau(k)$, defined as the time for a fluid element with energy $E(k)$ to move a distance $1/k$. So we have

$$\frac{1}{k} = U\tau(k)$$

But the scale velocity, U, is related to $E(k)$ by

$$E(k) = \frac{U^2}{k}$$

so τ is given by

$$\tau = \left(k^3 E(k)\right)^{-1/2} \tag{2.10}$$

If we assume that ϵ is a function only of k, τ and $E(k)$ the only dimensionally correct form for this is

$$\epsilon \sim \frac{kE(k)}{\tau(k)}$$

substituting in (2.10) again gives

$$E(k) = \kappa \epsilon^{2/3} k^{-5/3}$$

2.1.4 Forward enstrophy cascade region

We now consider the part of the energy spectrum dominated by transfer of enstrophy to larger wavenumbers. We denote the rate of transfer of enstrophy as η. This time we assume that the spectrum is determined only by k and η. The dimensionally correct scaling for η gives

$$\eta \sim \frac{k^3 E(k)}{\tau(k)}$$

Substituting in (2.10) gives

$$E(k) = \kappa \eta^{2/3} k^{-3}$$

Where κ is a constant.

So, the part of the energy spectrum dominated by energy transfer has a shape $k^{-5/3}$ and the part dominated by enstrophy transfer has a shape of k^{-3}.

2.2 Numerical Experiments

Figures 2.3 and 2.4 show the evolution of vorticity in an unforced channel model with constant f. The model was initialised with a thin wavenumber distribution of vorticity, centered at wavenumber eight.

The most notable feature in the initial (to ~ 70 hrs) evolution is the formation of thin "streamers" of vorticity. This implies that enstrophy is moving to larger wavenumbers (or smaller scales), as predicted. Later on the main feature is the organisation of vorticity into larger patches, i.e. lower wavenumber. The streamers produced early on in the evolution are mainly lost from about 300 hours, due to diffusion. This appears to serve to limit the transfer of vorticity to smaller scales. The formation of large eddies stops from about 500 hours; there appears to be a limit on the transfer of energy to larger scales. After 500 hours the eddies move around the system but rarely interact. From this point the system is dominated by diffusion.

2.2.1 Energy and Enstrophy Wavenumber Distributions

Figure 2.5 shows the 2D wavenumber distribution of energy as the model is initialised. Particularly notable is that the wavenumber distribution is quite close to being isotropic, i.e for a given k there is an approximately equal magnitude of $E(k)$ in each direction. One strange feature is the band of low numbers in k_x, extending across the k_y spectrum. Rather than being a feature of the turbulence I believe that this is Gibbs noise caused by the lack of periodicity in the y direction. This is discussed in Appendix A. The highest magnitudes occur at wavenumber ten.

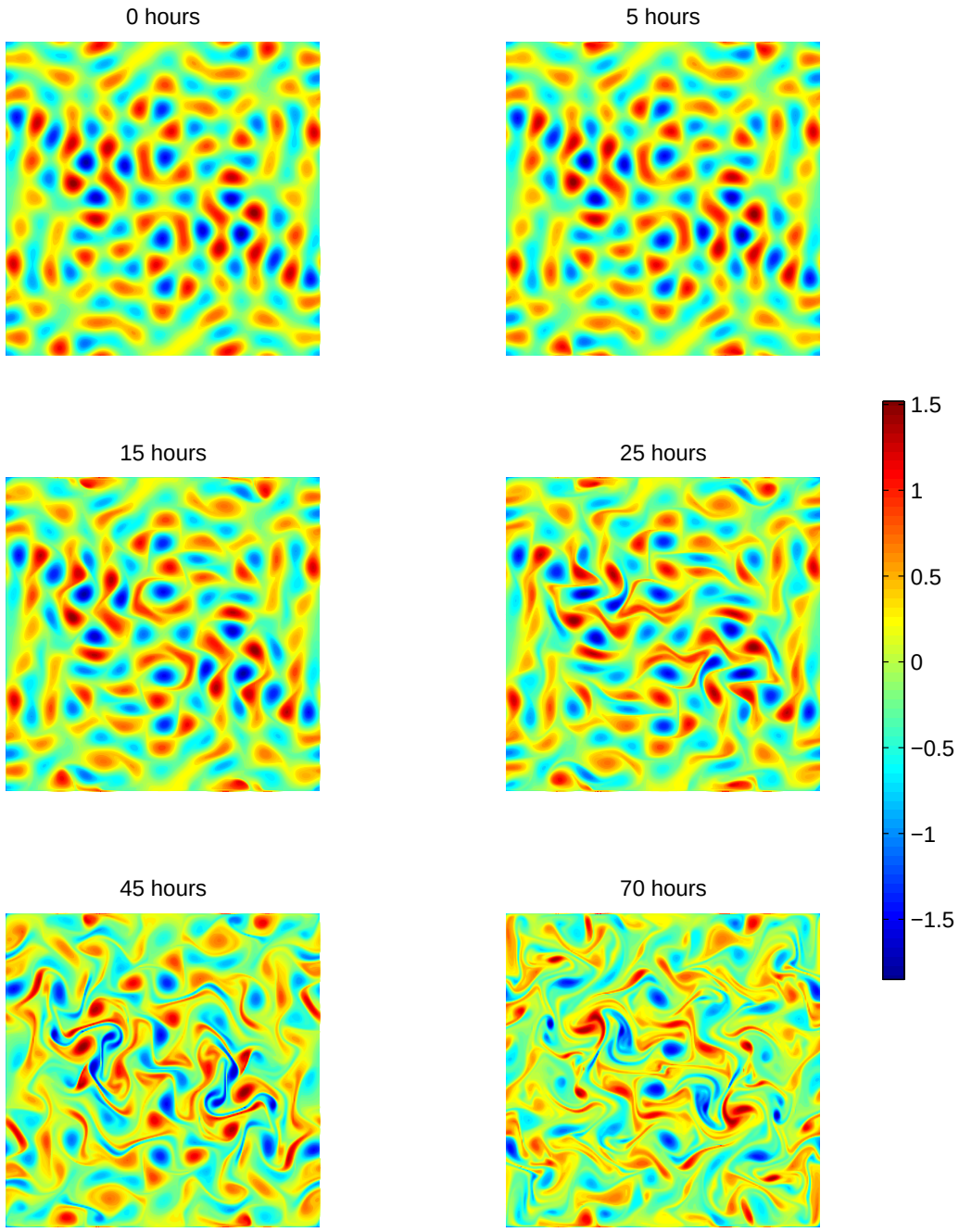

Figure 2.3: Evolution of vorticity on an f-plane. Scale is vorticity/f

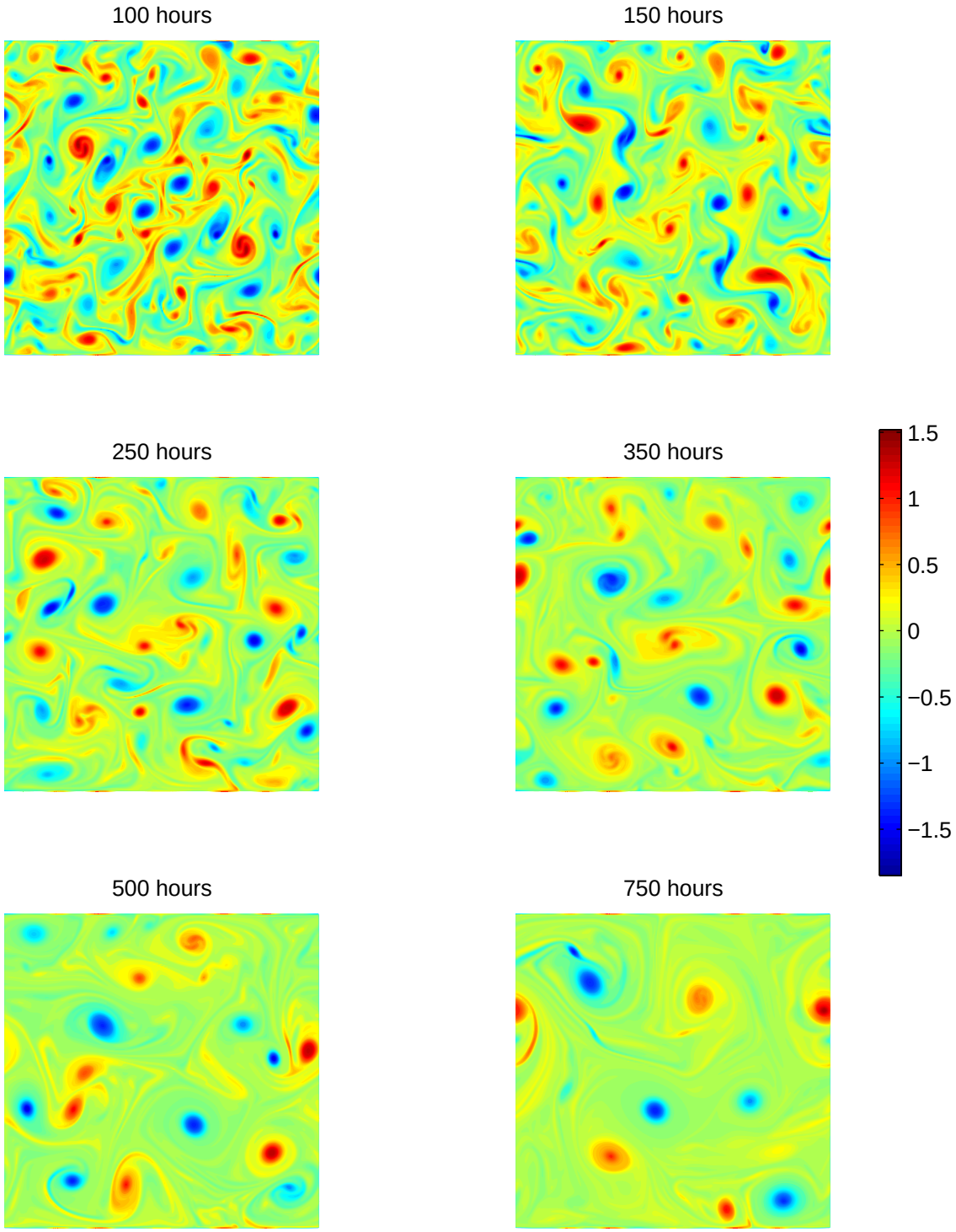

Figure 2.4: Evolution of vorticity on an f-plane. Scale is vorticity/f

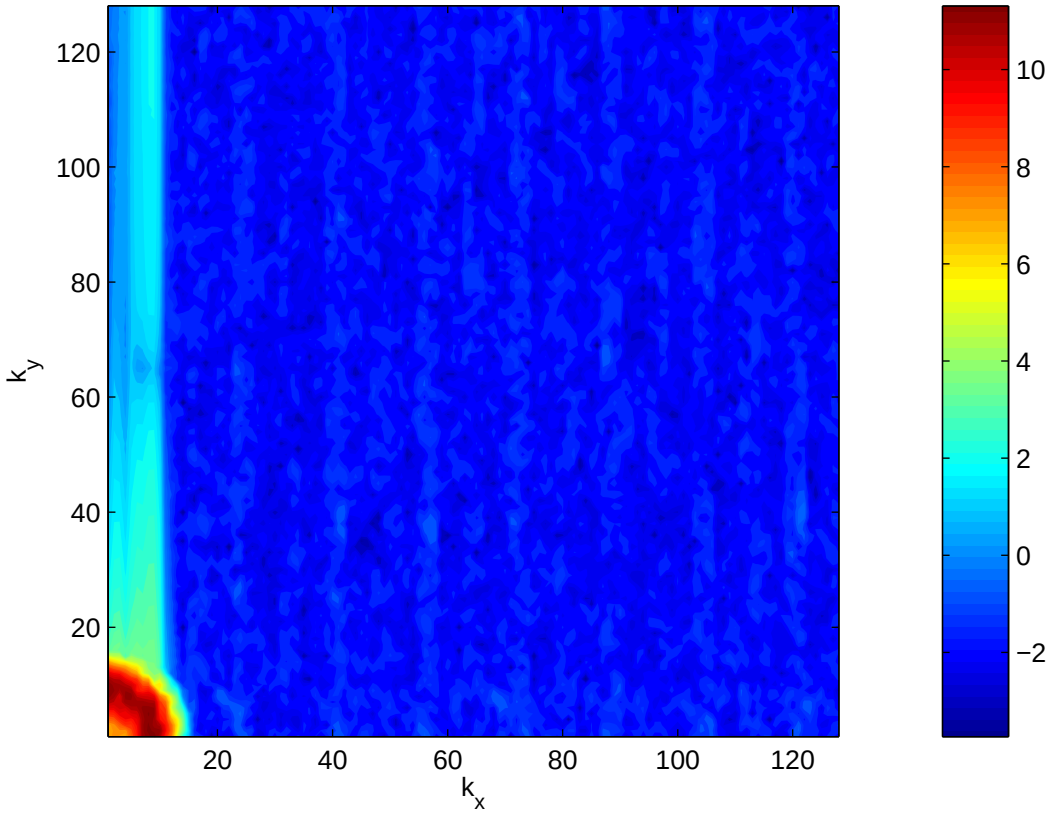

Figure 2.5: Initial wavenumber distribution of Energy on an f-plane scaled logarithmically

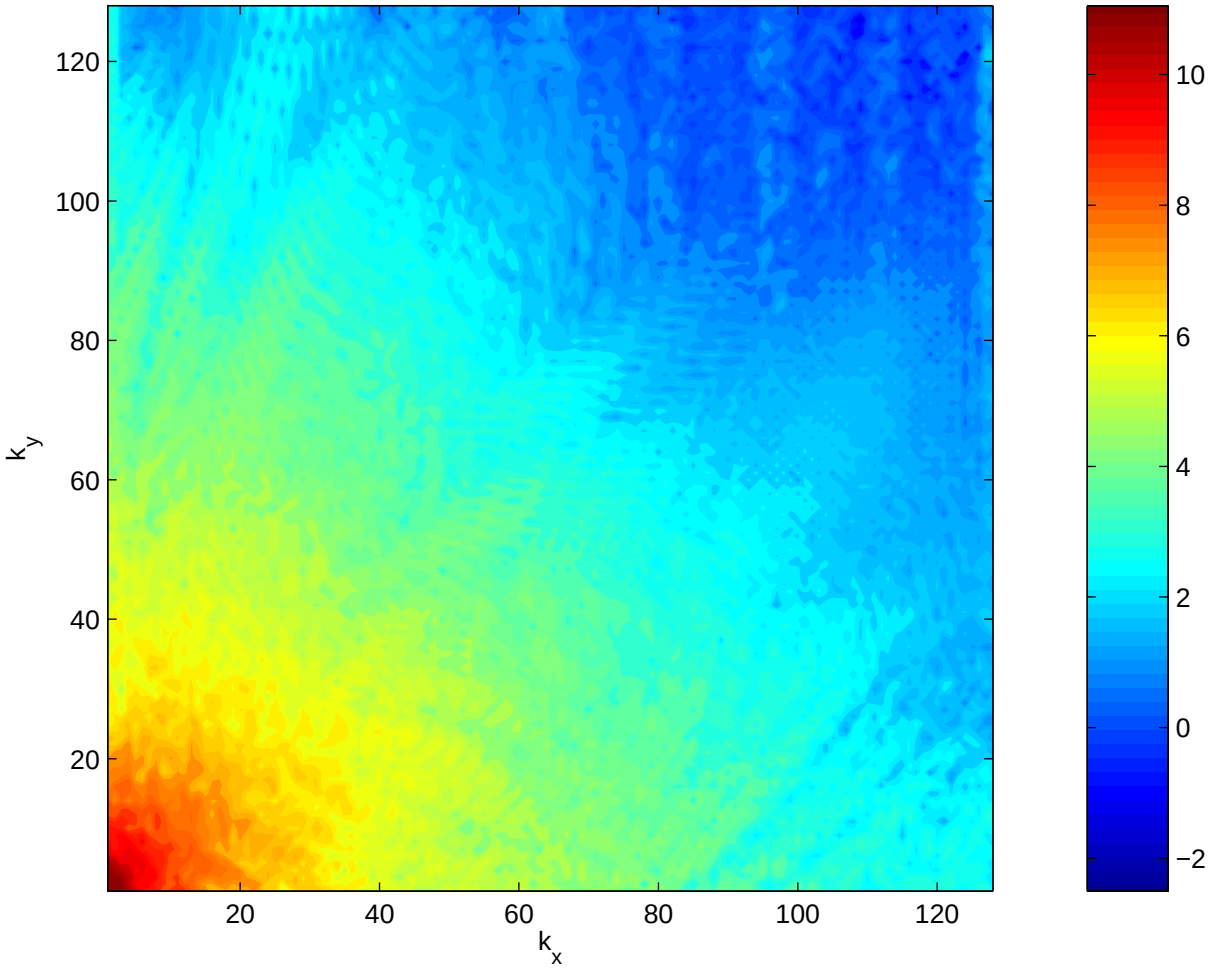

Figure 2.6: Average wavenumber distribution of Energy on an f-plane 500hrs to 750hrs scaled logarithmically

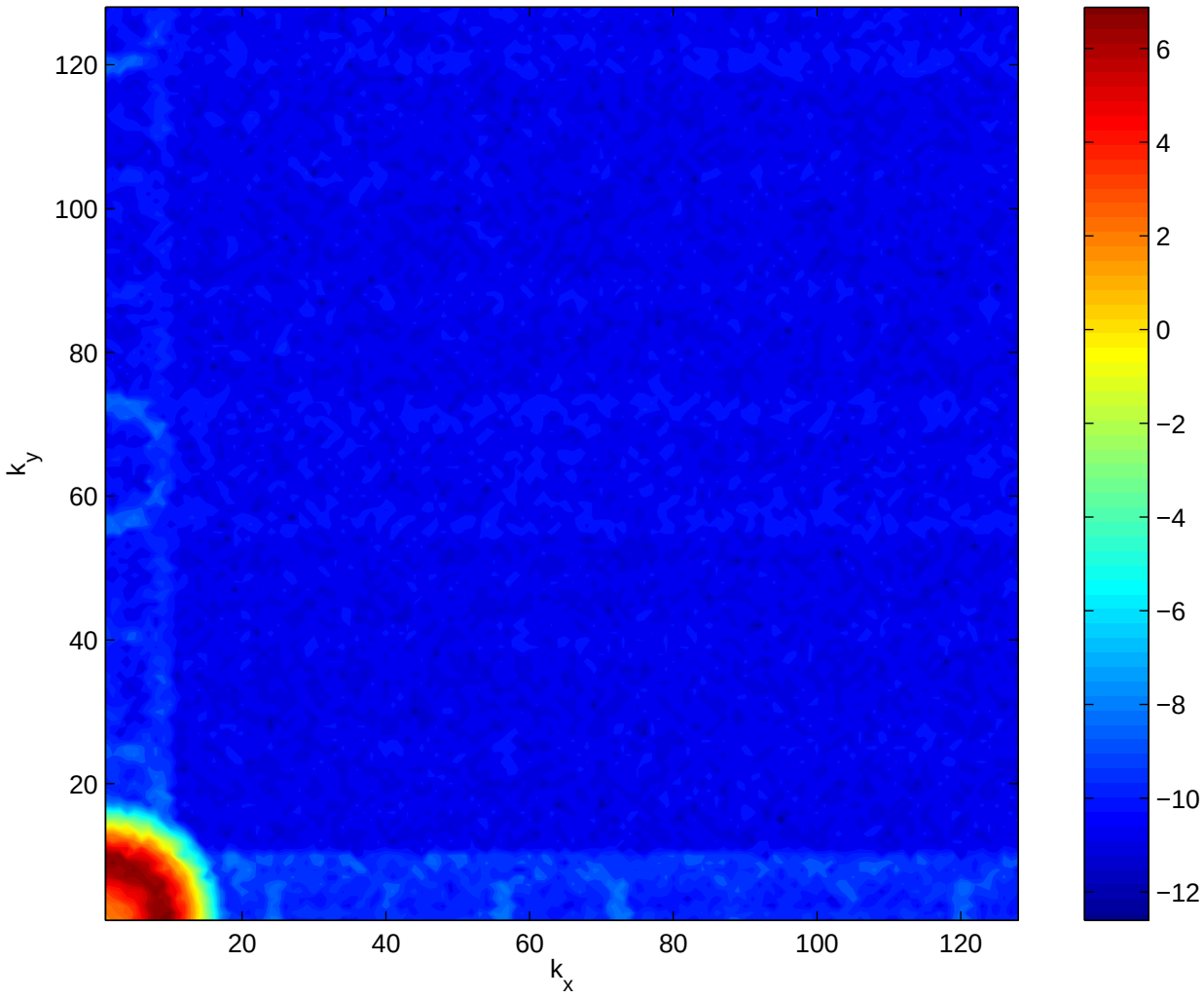

Figure 2.7: Initial wavenumber distribution of enstrophy on an f-plane scaled logarithmically

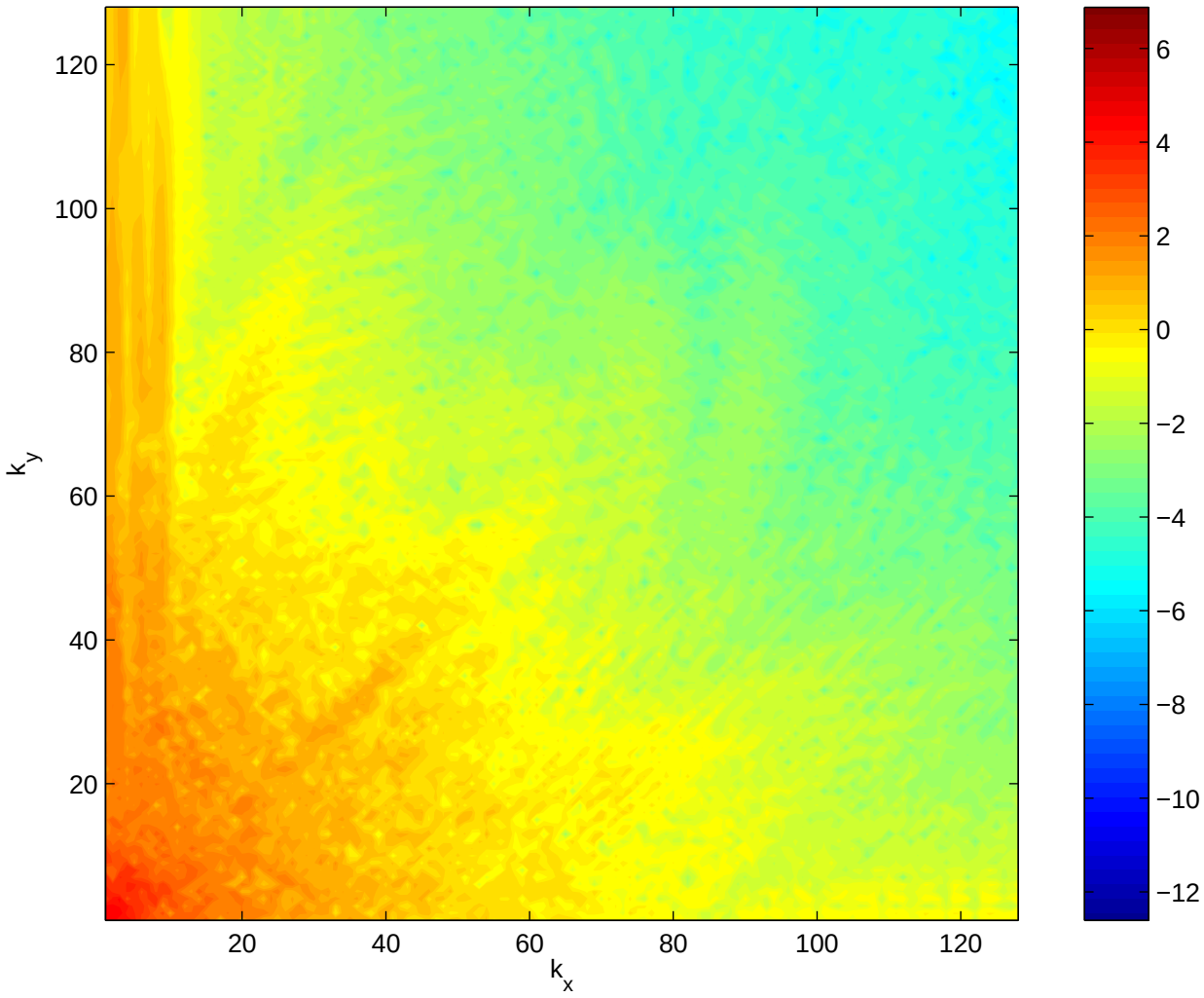

Figure 2.8: Average wavenumber distribution of enstrophy on an f-plane 500hrs to 750hrs scaled logarithmically

Figure 2.6 shows the 2D wavenumber distribution of energy, averaged from 250 to 750 hours. This shows a number of contrasts to 2.5. Most striking is that energy is now spread over a much wider range of wavenumbers. This appears to confirm the assumption that the wavenumber distribution would spread, made when deriving the properties of 2D turbulence. It is also notable, however, that the largest energy concentrations have moved to smaller wavenumbers compared to the initial peak at wavenumber eight. Although there are various details within the structure the averaged spectra remains broadly isotropic, especially at the highest energy concentrations.

Figure 2.7 shows the wavenumber initial distribution of enstrophy. This is almost perfectly isotropic and, as with the initial energy wavenumber distribution has the highest concentration at wavenumber eight.

Figure 2.8 shows the wavenumber distribution of enstrophy averaged between 250 and 750 hours. As with the energy wavenumber distributions there is a large spreading of enstrophy from small to large numbers. Unlike the energy distribution, the enstrophy distribution has less of a concentration of enstrophy at very small wavenumbers, implying there has been a shift of enstrophy from small to large wavenumbers.

2.2.2 Evolution of wavenumber profile

Figure 2.9 shows the isotropic wavenumber distribution of kinetic energy. These are calculated by summing the wavenumbers of each magnitude as described in [20].

The initial distribution is quite thin and is concentrated on wavenumber eight, due to the way the model is initialised. At 80 hours the fall of of energy concentration with wavenumber is approximately k^{-3}. Beyond this the fall steepens. This corresponds with the behaviour observed elsewhere, in particular [17]. This behaviour appears to be caused once the cascade hits a limit where the energy has collected into large vortices which then stop interacting.

Figure 2.10 shows the isotropic wavenumber distribution of enstrophy. It appears that the enstrophy is spread over a far wider range of wavenumbers than the energy spectrum.

2.2.3 Evolution of mean wavenumber of energy and enstrophy

Figure 2.11 shows the evolution of the mean wavenumber of energy and enstrophy, calculated using (2.6).

Considering first the energy profile, this starts at wavenumber eight and rapidly decreases as predicted by 2D turbulence theory. This lasts for about 300 hours. Beyond this the decay is only very slight and the system settles to

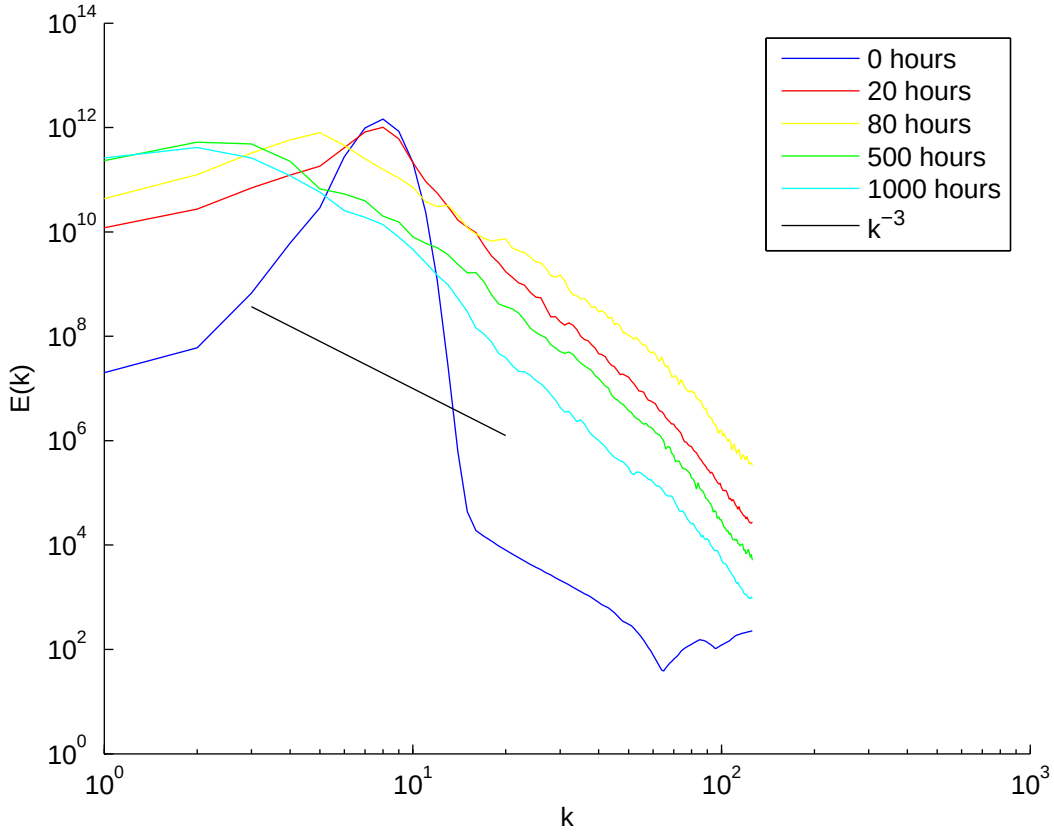

Figure 2.9: Evolution of wavenumber distribution of kinetic energy

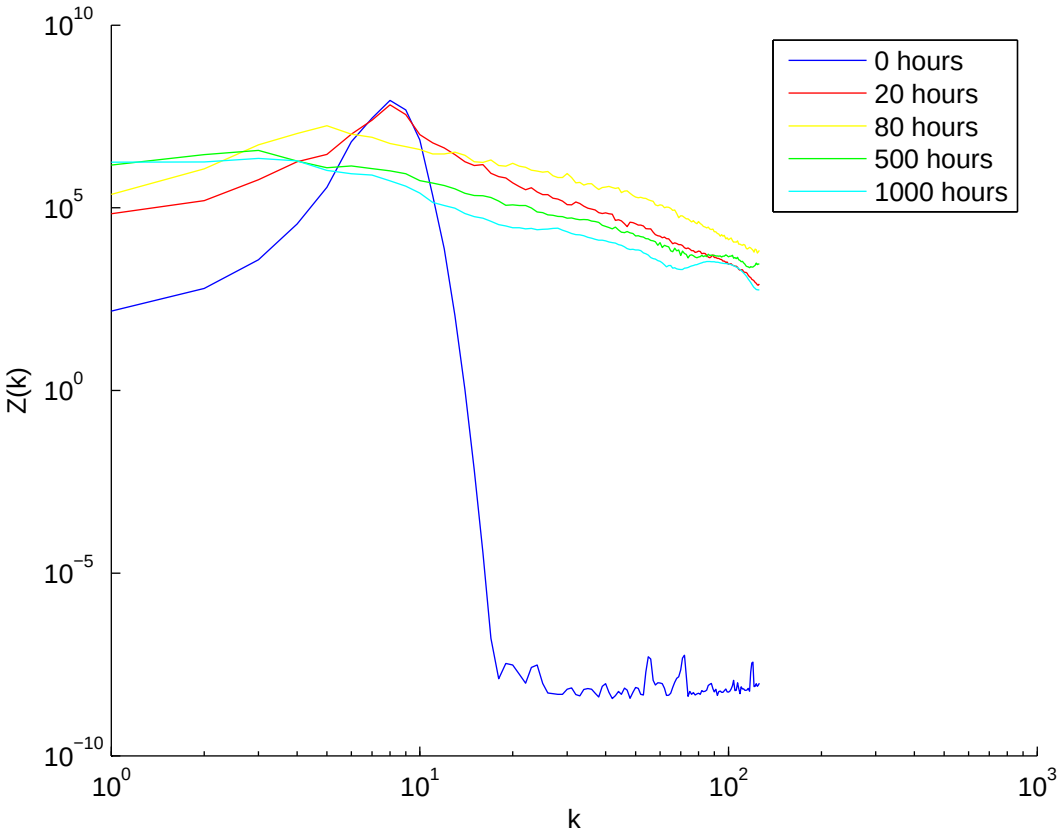

Figure 2.10: Evolution of wavenumber distribution of enstrophy

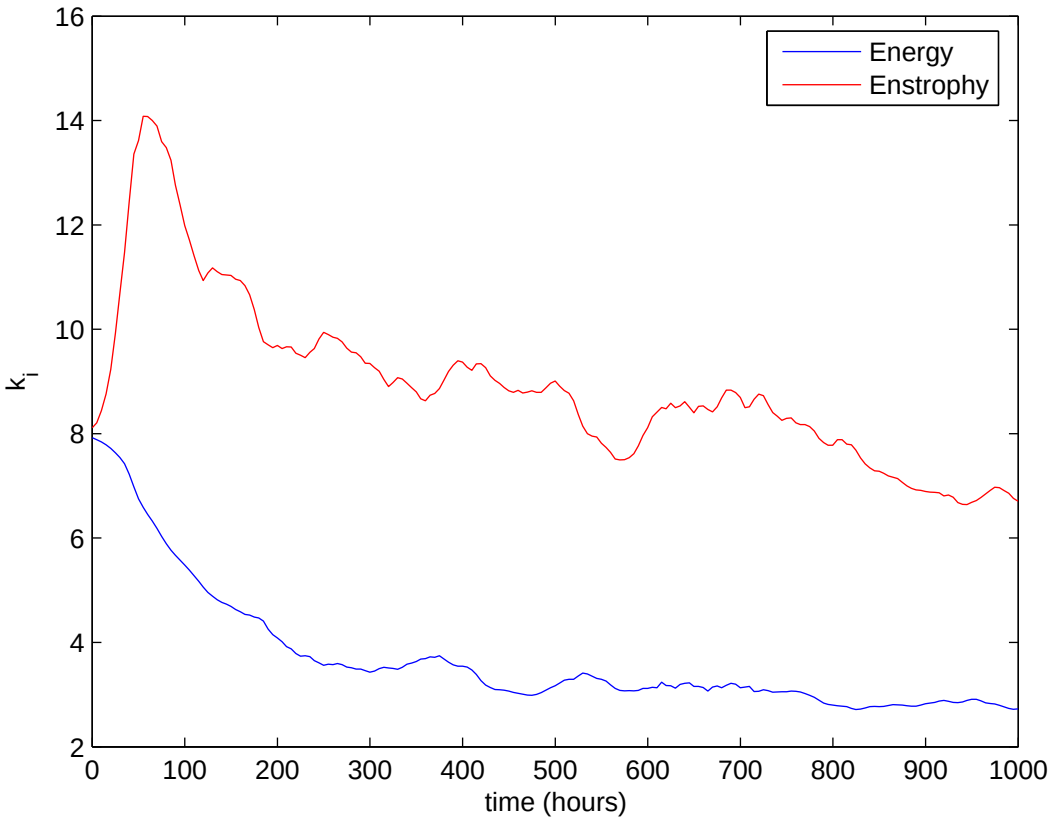

Figure 2.11: Evolution of mean wavenumber of energy and enstrophy

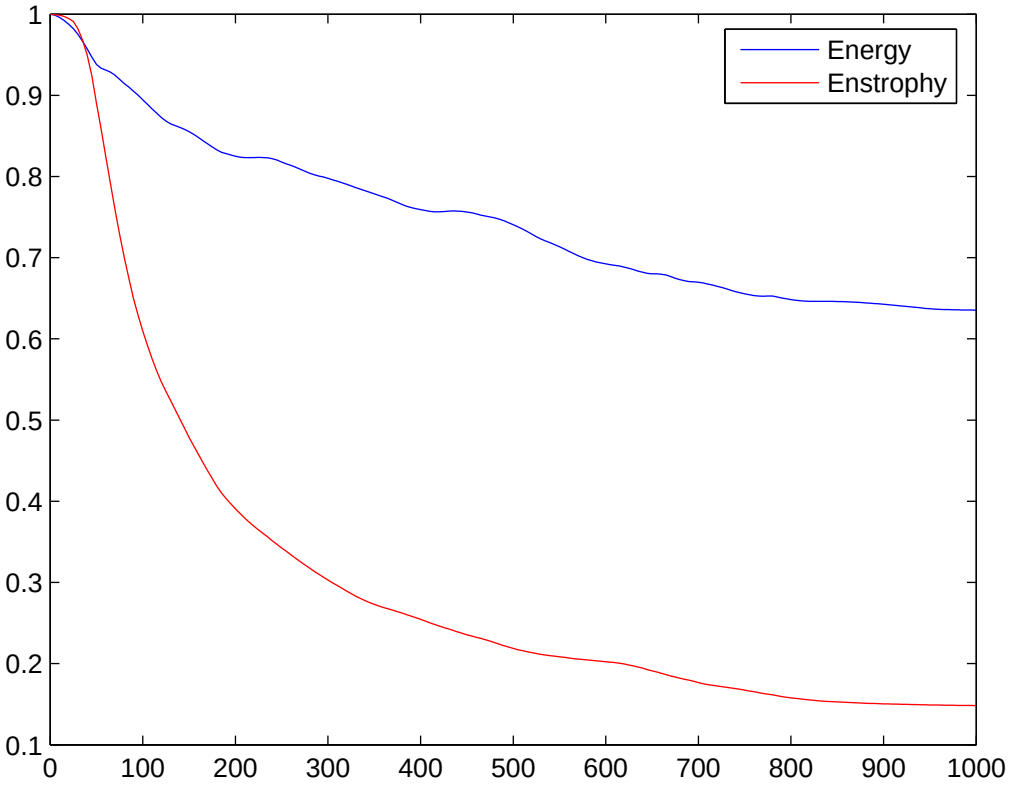

Figure 2.12: Normalised evolution of total energy and enstrophy

a steady mean wavenumber of approximately three. This corresponds to the organisation of the flow into large eddies which stops when some limit is reached.

The enstrophy profile shows initially a sharp rise, lasting for 75 hours. This corresponds to the formation of thin "streamers" of vorticity in the flow. After 75 hours there is a rapid change in the dynamics of the enstrophy change and enstrophy is transferred to smaller wavenumbers. This continues for the remainder of the model run. The abruptness of this change is somewhat remarkable. This may be due to fine vorticity structures being particularly susceptible to diffusion. At the same time, because the system is loosing energy, the rate at which these structures may be produced is dramatically reduced.

2.2.4 Conservation of Energy and Enstrophy

Figure 2.12 shows the change of total energy and enstrophy in the system. This shows that neither energy nor enstrophy are actually conserved as in an idealised system. The energy, however is lost relatively slowly; ($\sim$ 65%) of the initial energy remains in the system after 1000 hours. Meanwhile the enstrophy is lost far more rapidly than energy. This because most of the vorticity (and therefore enstrophy) resides in very small scale structures which are more susceptible to dissipation by diffusion. Although diffusion is not explicitly included it is a feature of semi-Lagrangian schemes. This is discussed further in Appendix A.

Chapter 3

Beta Turbulence

In the previous chapter we investigated the properties of two dimensional turbulence, that is turbulent flow in a domain with constant Coriolis parameter. We now consider the effect of a linearly varying f on the evolution of turbulent motion.

Considering a beta plane approximation, Taylor's result that the absolute vorticity is conserved holds but since the planetary vorticity is no longer constant the relative vortiticy is not conserved. Absolute vortiticy, ζ is given by $\zeta = \xi + f$ where f is given by $f = \beta y$, β being constant for a beta plane. Hence (2.1) becomes

$$\frac{D}{Dt}\left(\xi + \beta y\right) = 0 \tag{3.1}$$

Expanding this gives

$$\frac{\partial \xi}{\partial t} + \boldsymbol{u}.\bigtriangledown \xi + \beta v = 0 \tag{3.2}$$

For the case that the nonlinear term in (3.2), $\boldsymbol{u}.\bigtriangledown \xi$, is negligibly small, arbitrary initial values of streamfunction may be decomposed into a series of *Rossby waves* [19]. As the governing equation is now linear, the evolution of these waves may be predicted simply.

This can also be expressed in terms of conservation of a potential vortiticy, q, where $q = \xi + \beta y$.

3.1 The Rossby Wave

The idea of describing flow evolution in terms of a wave equation was first presented by Rossby but is now reproduced in numerous review papers, and text books. The derivation presented here follows the form of that given by [7].

The flow is written as a base zonal flow, $U(y)$, which varies with latitude plus perturbations which vary in time so

$$\boldsymbol{u} = \left(U + u\left(t\right)\right)\boldsymbol{i} + v\left(t\right)\boldsymbol{j}$$

where $\boldsymbol{i}$ and $\boldsymbol{j}$ are unit vectors in the zonal and meridional directions, respectively. We also define a perturbation streamfunction, ψ, such that

$$u = -\frac{\partial \psi}{\partial y}$$

and

$$v = \frac{\partial \psi}{\partial x}$$

We also have

$$\xi = \bigtriangledown^2 \psi$$

If we now rewrite (3.2) in terms of ψ, ignoring products of perturbation quantities, we have

$$\frac{\partial}{\partial t} \bigtriangledown^2 \psi + U \frac{\partial}{\partial x} \bigtriangledown^2 \psi + \beta \frac{\partial \psi}{\partial x} = 0 \tag{3.3}$$

which has solutions of the form

$$\psi = \mathrm{Re}\left(Z e^{i(k_x x + k_y y - \omega t)}\right)$$

where k_x, k_y are wavenumbers, Z is the amplitude and ω is the frequency. The frequency is given by

$$\omega = -\frac{\beta k_x}{k_x^2 + k_y^2} \tag{3.4}$$

The phase speed, relative to the mean flow is given by

$$c_p = \frac{\omega}{k_x}$$

This means that the waves are dispersive - the phase speed is dependent on wavenumber. Lower number wavenumbers propagate more rapidly than high wavenumbers.

3.2 The Mixed Case

In reality flows on a beta plane will contain both turbulent and wave characteristics. We now consider the energy and enstrophy properties of such flows.

3.2.1 Conversion of Waves to Turbulence

Scaling argument

Vallis provides[25] a scaling argument describing whether waves or turbulence will dominate at a particular scale.

Firstly we scale (3.2) using L for a scale length, U for a scale velocity and T as a time scale. This gives

$$\frac{\partial \xi}{\partial t} + \boldsymbol{u}.\bigtriangledown \xi + \beta v = 0$$
$$\frac{U}{LT} + \quad \frac{U^2}{L^2} + \beta U = 0$$

We wish to establish whether $\frac{\partial \xi}{\partial t}$ is dominated by the non linear term or by the Rossby wave term. By considering the ratio of these two terms we establish a wave turbulence boundary scale length, L_β

$$L_\beta = \sqrt{\frac{U}{\beta}} \tag{3.5}$$

Motions which occur at scales larger than L_β will tend to be dominated by the Rossby wave term, whereas motions occurring at smaller scales will tend to be dominated by the non linear term. This is more commonly expressed as a wave turbulence boundary wavenumber

$$k_\beta = \sqrt{\frac{\beta}{U}} \tag{3.6}$$

which is scaled by the size of the domain.

Eddy turnover time argument

A slightly more rigorous derivation of the wave turbulence boundary scale may be made using a similar argument to that used to derive inertial ranges. This is done by equating the eddy turnover time to the reciprocal of the Rossby wave frequency (3.4). The eddy turnover time from (2.10) is given by

$$\tau(k) = \epsilon^{-1/3} k^{-2/3}$$

Equating this to 1/(3.4), taking the case that $k_x = k_y$, gives

$$k_\beta = \left(\frac{\beta^3}{\epsilon}\right)^{\frac{1}{5}} \tag{3.7}$$

The disadvantage of this form is that estimating the energy transfer rate is non trivial, even for a numerical model; in practice it would be much easier to make calculations using (3.5) or (3.6) than (3.7). The advantage, however is that it makes explicit the relationship between k_β and β. The energy flux is unlikely to

be a function of β for a system in equilibrium, whereas the r.m.s velocity is likely to be a function of β.

Figure 3.1 illustrates the effect of adding a β field to the energy wavenumber distribution. The most notable change from the two dimensional turbulence case is that the peak in energy occurs at wavenumber k_β rather than at $k = 1$. Energy supplied to the centre of the spectrum is cascaded toward lower wavenumbers, however once k_β is reached the energy transfer is inhibited.

3.2.2 Generation of Anisotropy

We have so far assumed that the wave turbulence boundary is isotropic, yet this is further not the case, the frequency of Rossby waves being given by (3.4). The anisotropy of Rossby waves is further confirmed by observations of the atmosphere and by numerical models. Quantifying the wave turbulence boundary was first proposed by Rhines[19] and later expanded by Vallis[25].

We adopt a similar procedure to that used whilst determining the isotropic wave turbulence boundary, equating the reciprocal of the Rossby wave frequency to the eddy turnover time, however this time we do not equate k_x and k_y. Noting that $k_x^2 + k_y^2 = k^2$ we have

$$\epsilon^{1/3} k^{2/3} = -\frac{\beta k_x}{k^2}$$

This has solutions for $k_{x\beta}$ and $k_{y\beta}$ of

$$k_{x\beta} = \left(\frac{\beta^3}{\epsilon}\right)^{1/5} \cos^{8/5}\theta \tag{3.8}$$

$$k_{x\beta} = \left(\frac{\beta^3}{\epsilon}\right)^{1/5} \sin\theta \cos^{3/5}\theta \tag{3.9}$$

Where θ represents the angle between k_x and k_y.

This is simplified by parameterising the turbulence frequency as Uk which gives solutions

$$k_{x\beta} = \left(\frac{\beta}{U}\right)^{1/2} \cos^{3/2}\theta \tag{3.10}$$

$$k_{x\beta} = \left(\frac{\beta}{U}\right)^{1/2} \sin\theta \cos^{1/2}\theta \tag{3.11}$$

3.3 Numerical Experiments

3.3.1 Evolution of flow on a beta plane

Figure 3.2 shows the effect of varying β on the evolution of vorticity. For the low β case, the flow is dominated by the nonlinear term and the flow is essen-

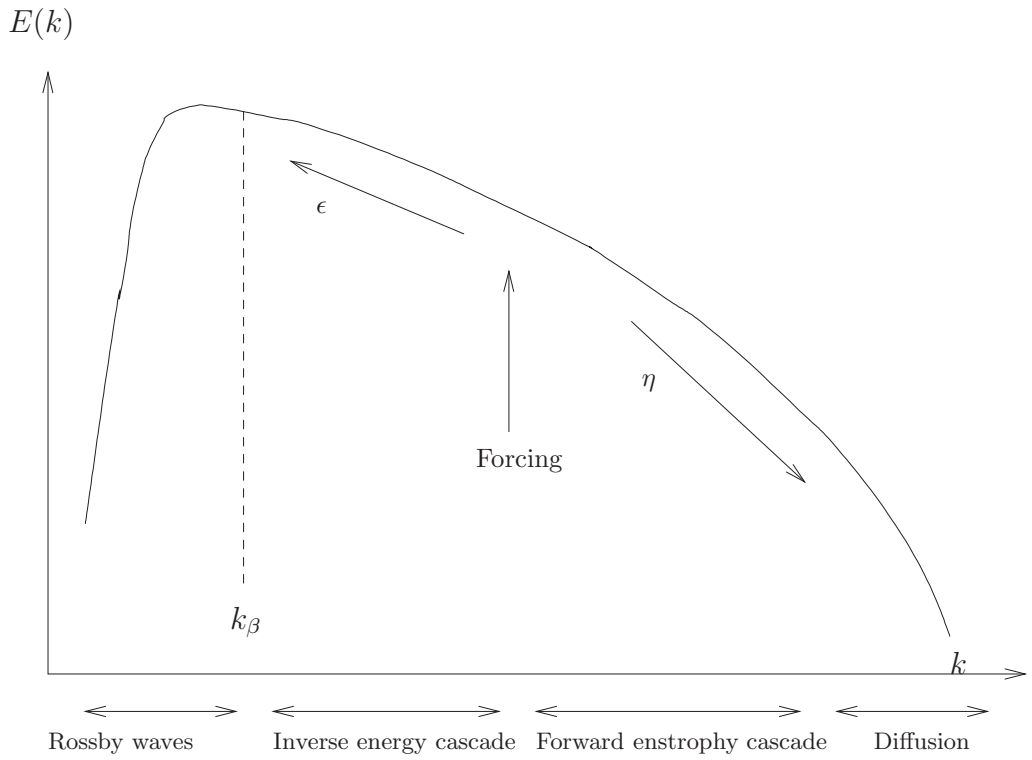

Figure 3.1: Idealised isotropic energy and enstrophy spectrum in barotropic β plane turbulence. Source: [26].

tially that described in the two dimensional turbulence. The energy wavenumber distribution remains isotropic.

In the middle case, the flow is still similar to that observed in the turbulent case however there is a notable zonal elongation of the eddies. There is also a corresponding elongation of the energy spectra in the k_y direction.

For the high β case the flow is dominated by waves. The eddies are highly elongated in the zonal direction and there is a strong corresponding stretching of the energy spectrum in the k_y direction. The other notable feature is that the peak in the energy spectra is at approximately wavenumber ten. This is because motions at scales with wavenumbers lower than this are dominated by the linear term, this has the effect of interrupting the transfer of energy from small to large scales normally associated with two dimensional turbulence.

Figure 3.3 shows a vorticity field in a flow in which the wave term dominates. The wave turbulence boundary wavenumber is approximately 10. It is particularly apparent that the eddies are elongated in the zonal direction. Figure 3.4 shows the corresponding energy wavenumber distribution.

3.3.2 Evolution of wavenumber distribution

Figure 3.5 shows the time evolution of isotropic wavenumber. Comparing this with the case for two dimensional turbulence (Figure 2.9), the peak energy distribution is at a much higher wavenumber than for the two dimensional turbulence case.

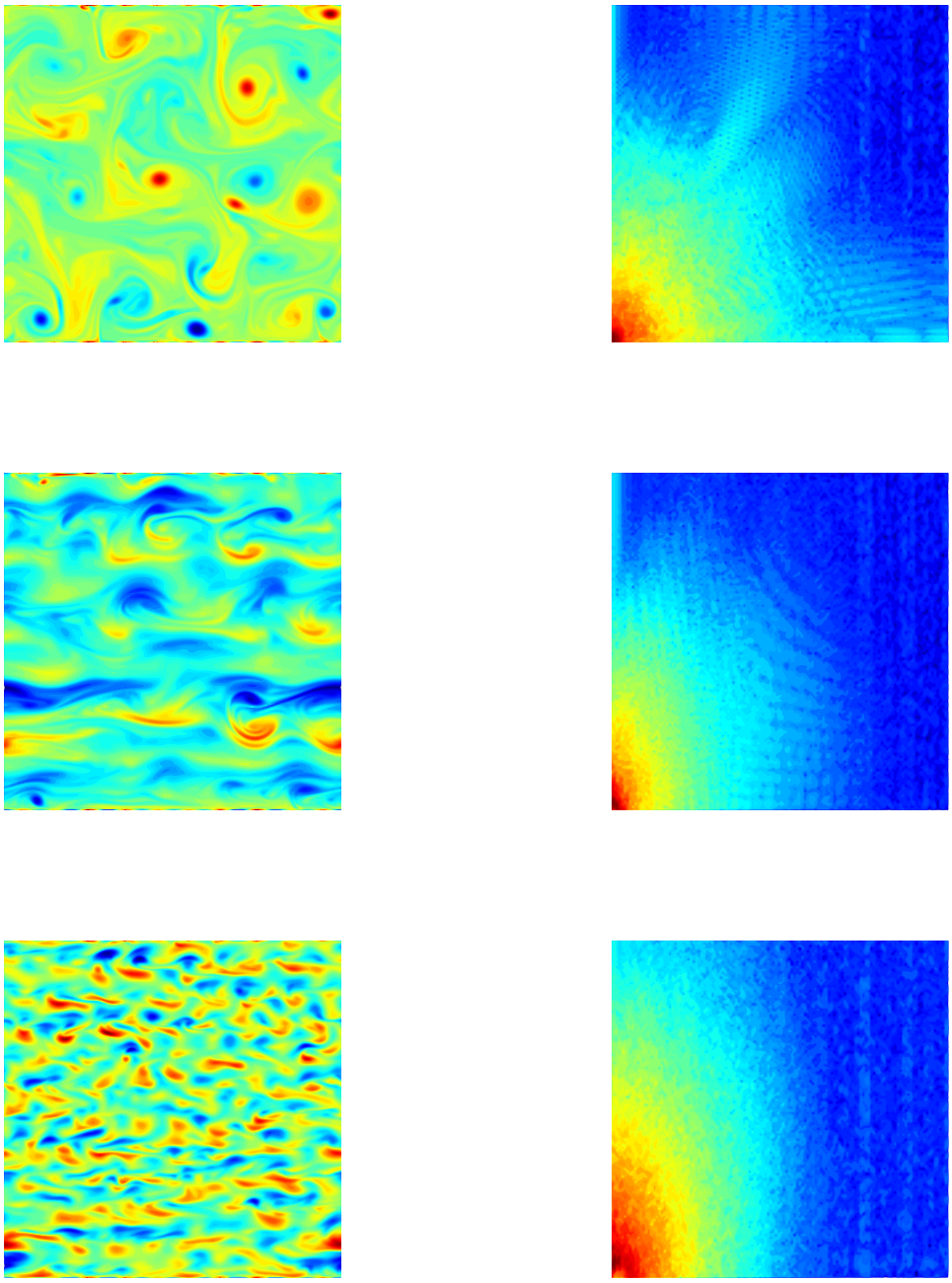

Figure 3.2: Vorticity (left) and energy spectra (right) for different values for β. Top: High latitude case, $k_\beta < 1$. Middle row: Mid latitude, $k_\beta = 3$, Low latitude, high β case, $k_\beta = 10$. All the plots were initialised with a thin wavenumber distribution of vorticity, centred at wavenumber ten.

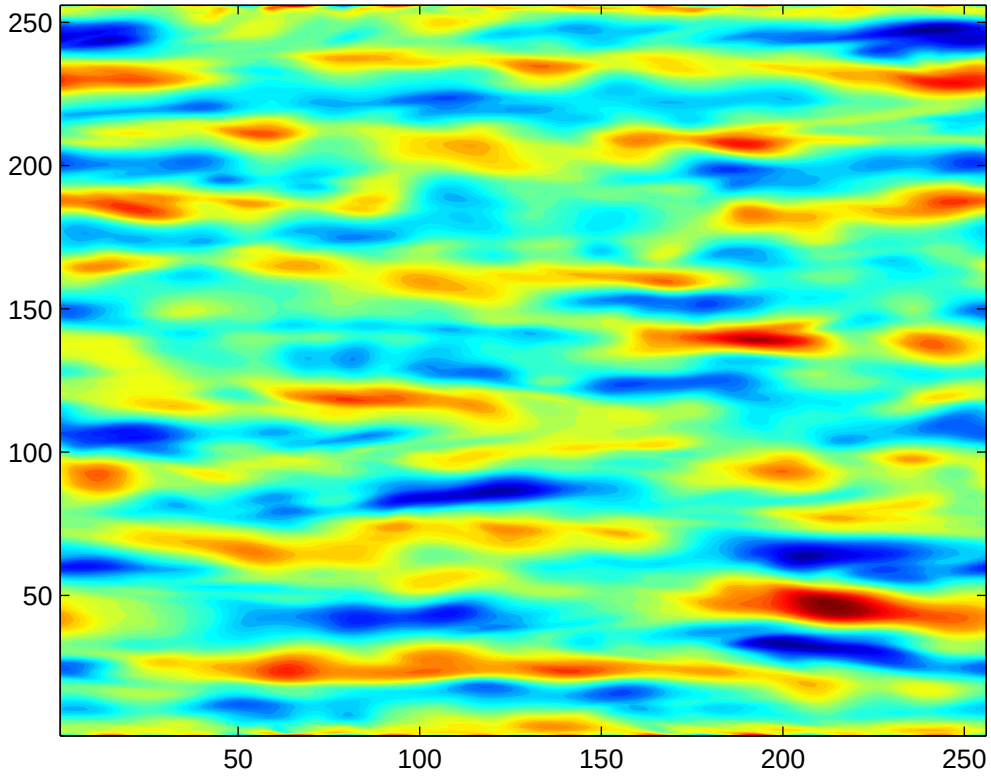

Figure 3.3: Vorticity after 1000 hours (high β)

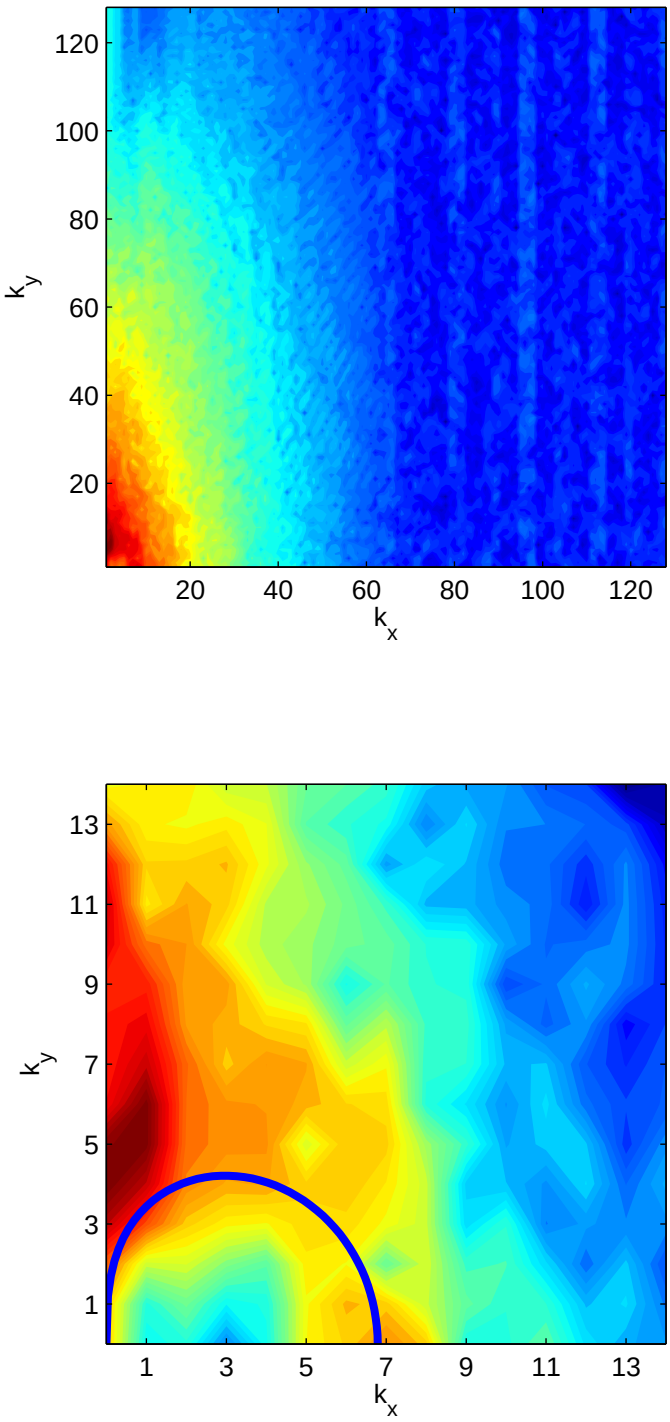

Figure 3.4: Energy wavenumber distribution after 1000 hours (high β). Lower panel shows the structure of lower wavenumbers more clearly; The thick blue line shows the wave turbulence boundary calculated using (3.11) and (3.11)

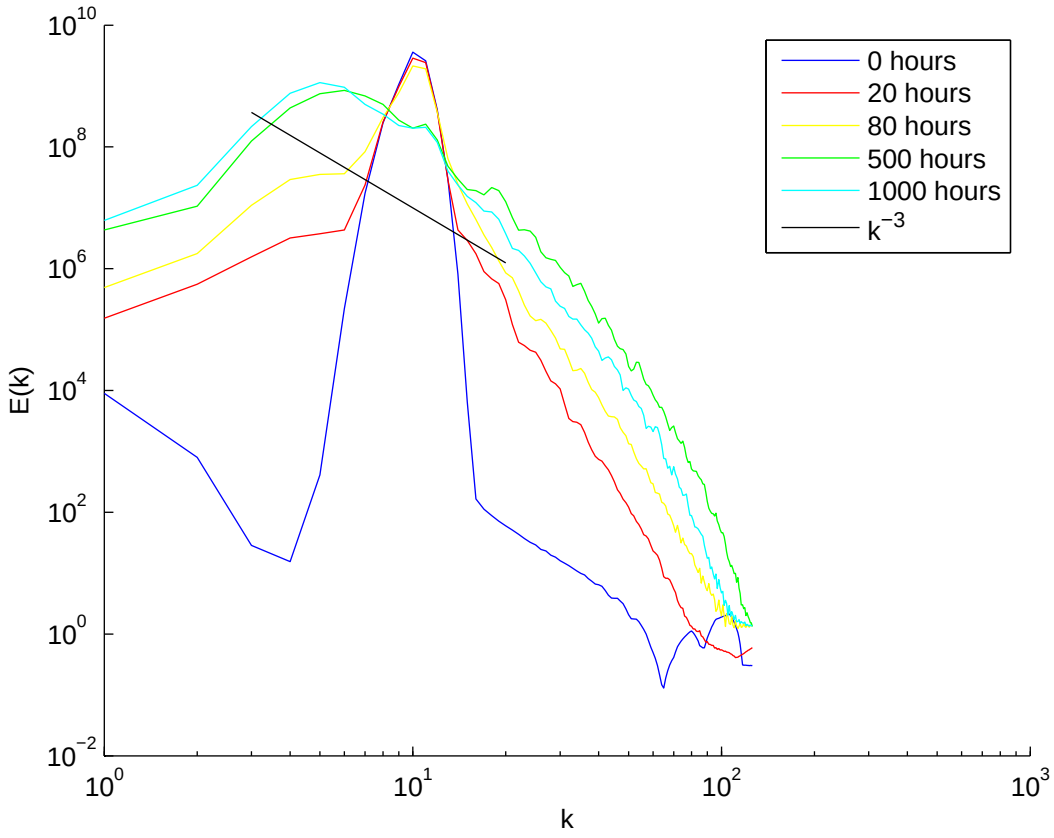

Figure 3.5: Evolution of isotropic energy spectrum (high β)

Chapter 4

Effect of Orography

4.1 The effect of orography

We have so far considered the evolution of turbulent flow on both an f-plane and a beta-plane, for the case that the fluid is within a flat channel. We now consider the case that the bottom of the channel has shallow orography. The description shallow implies that the orography acts to compress the flow above it but does not actually obstruct the flow.

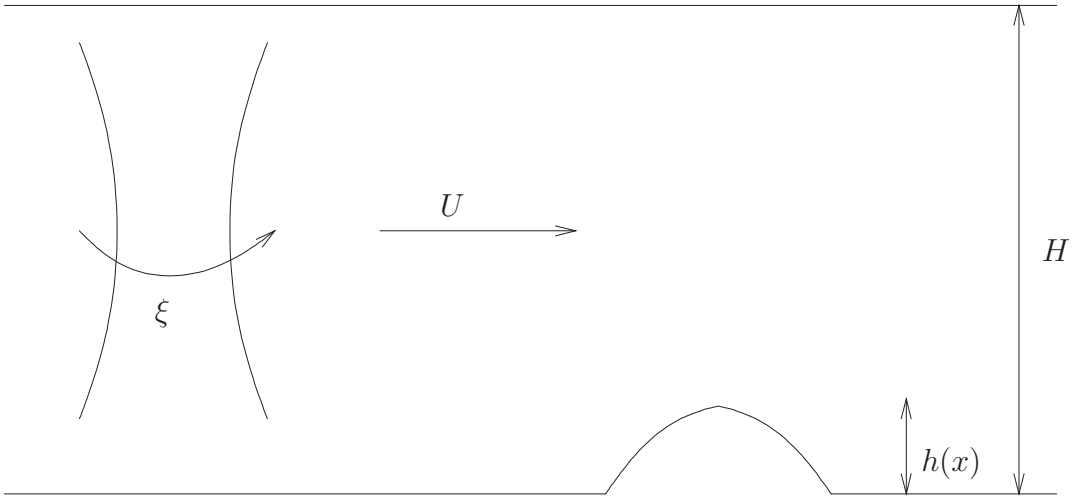

Figure 4.1: Schematic effect of orography on two dimensional flow

Consider a vortex in a two dimensional flow being moved over a shallow (relative to the depth of the flow) "hill" (Figure 4.1). As the vortex moves over the hill it will become squashed, changing the rate of rotation through conservation of momentum. We now attempt to express this in terms a vorticity equation.

The vorticity form of the Euler momentum equation is

$$\frac{\mathrm{D}\boldsymbol{\zeta}}{\mathrm{D}t} = \frac{\bigtriangledown\rho \times \bigtriangledown p}{\rho^2} + \boldsymbol{\zeta}.\bigtriangledown \boldsymbol{u} - \boldsymbol{\zeta}(\bigtriangledown.\boldsymbol{u})$$

If we now consider a flow which is barotropic (so $\bigtriangledown\rho\times\bigtriangledown p = 0$) and the horizontal part of $\boldsymbol{u}$ does not vary with height (so $\frac{\partial u}{\partial z} = \frac{\partial v}{\partial z} = 0$) and is incompressible, we obtain an expression for the vertical component of $\boldsymbol{\zeta}$.

$$\frac{\mathrm{D}\zeta}{\mathrm{D}t} = (\xi + f)\frac{\partial w}{\partial z}$$

where ζ is the absolute vorticity, i.e. $\xi + f$ and w is the vertical velocity. If we take an f-plane approximation this gives

$$\frac{\mathrm{D}\xi}{\mathrm{D}t} = (\xi + f)\frac{\partial w}{\partial z}$$

Since $\xi \sim \frac{U}{fL} = Ro$ for low Rossby number flow we have

$$\frac{\mathrm{D}\xi}{\mathrm{D}t} = f\frac{\partial w}{\partial z}$$

If the top and bottom of the channel are parallel w will be zero throughout the fluid giving

$$\frac{\mathrm{D}\xi}{\mathrm{D}t} = 0$$

If, however, we introduce a variable height $h(x, y)$ of the lower boundary we still require $w = 0$ at the upper boundary but in order for flow to be parallel to the lower boundary we require $w = \boldsymbol{u}.\bigtriangledown h$. We can therefore approximate $\frac{\partial w}{\partial z}$ with $\frac{-\boldsymbol{u}.\bigtriangledown h}{H}$. Therefore we have

$$\frac{\mathrm{D}\xi}{\mathrm{D}t} = -\frac{f}{H}\boldsymbol{u}.\bigtriangledown h \tag{4.1}$$

This can also be expressed in terms of potential vorticity conservation

$$\frac{\mathrm{D}q}{\mathrm{D}t} = 0$$

where, for an f-plane, $q = \xi + \frac{fh}{H}$. We can check this by considering the Lagrangian derivative of q

$$\begin{aligned} 0 &= \frac{\mathrm{D}}{\mathrm{D}t}\left(\xi + \frac{fh}{H}\right) \\ &= \frac{\mathrm{D}\xi}{\mathrm{D}t} + \frac{\mathrm{D}}{\mathrm{D}t}\left(\frac{fh}{H}\right) \\ &= \frac{\mathrm{D}\xi}{\mathrm{D}t} + \frac{\partial}{\partial t}\left(\frac{fh}{H}\right) + \boldsymbol{u}.\bigtriangledown\left(\frac{fh}{H}\right) \\ &= \frac{\mathrm{D}\xi}{\mathrm{D}t} + \frac{f}{H}\boldsymbol{u}.\bigtriangledown h \end{aligned}$$

which is equal to (4.1).

4.2 Numerical Experiments

4.2.1 Effect of orography on an f-plane

Figure 4.2 shows the evolution of vorticity in a domain with a Gaussian hill at the centre which has a maximum height of 1/4 of the depth of the fluid. As the flow is zonal initially this means that ξ is zero across the domain. In terms of PV we have $q = \xi + \frac{fh}{H}$, hence there is a positive PV anomaly over the hill. As the positive anomaly moves away from the hill this results in an area of positive vorticity which will be advected across the domain. As fluid with PV=0 moves onto the hill, in order to conserve PV, this requires the establishment of negative vorticity (i.e. an anticyclone) above the hill. Hence we have an area of positive vorticity starting at the hill and gradually drifting round the domain and a permanent anticyclone over the hill.

4.2.2 Effect of Orography on a beta-plane

Figure 4.4 shows the evolution of vorticity on a beta plane. The initial evolution is similar to that in the f-plane case; a patch of positive vorticity leaves the hill and there is a permanent patch of negative vorticity over the hill. Beyond this, however, the evolution becomes more complex and can be best understood in terms of PV perturbations. Figure 4.3 gives a schematic of the evolution.

In Figure 4.3a a positive and negative vorticity patch are established as in the f-plane case. This has the effect of moving fluid meridionally; from north to south between the vortices and from south to north at the right hand end. Away from the hill we have $q = \xi + \beta y$, so when fluid is drawn north maintaining PV requires negative vorticity to be created and fluid drawn south creates positive vorticity. Therefore Figure 4.3b shows the creation of an additional patch of negative. This is repeated and a wave propagates across the domain (Figure 4.3c).

So, the hill causes a barotropic Rossby wave to propagate round the domain toward the east. When this wave has propagated right round the domain it causes an interference pattern and appears to result in turbulent behaviour.

Figure 4.5 shows the kinetic energy spectrum for this flow. There is a notable elongation of the spectra in the meridional direction, however there is no distinct wave-turbulence boundary.

4.2.3 Effect of orography on turbulent flow on an f-plane

Figure 4.6 shows the evolution of vorticity initialised with a thin wavenumber distribution of vorticity centred at wavenumber ten plus a zonal flow. Although there is clearly a patch of negative vorticity above the hill the addition of the hill does otherwise appear to affect the characteristics of the flow.

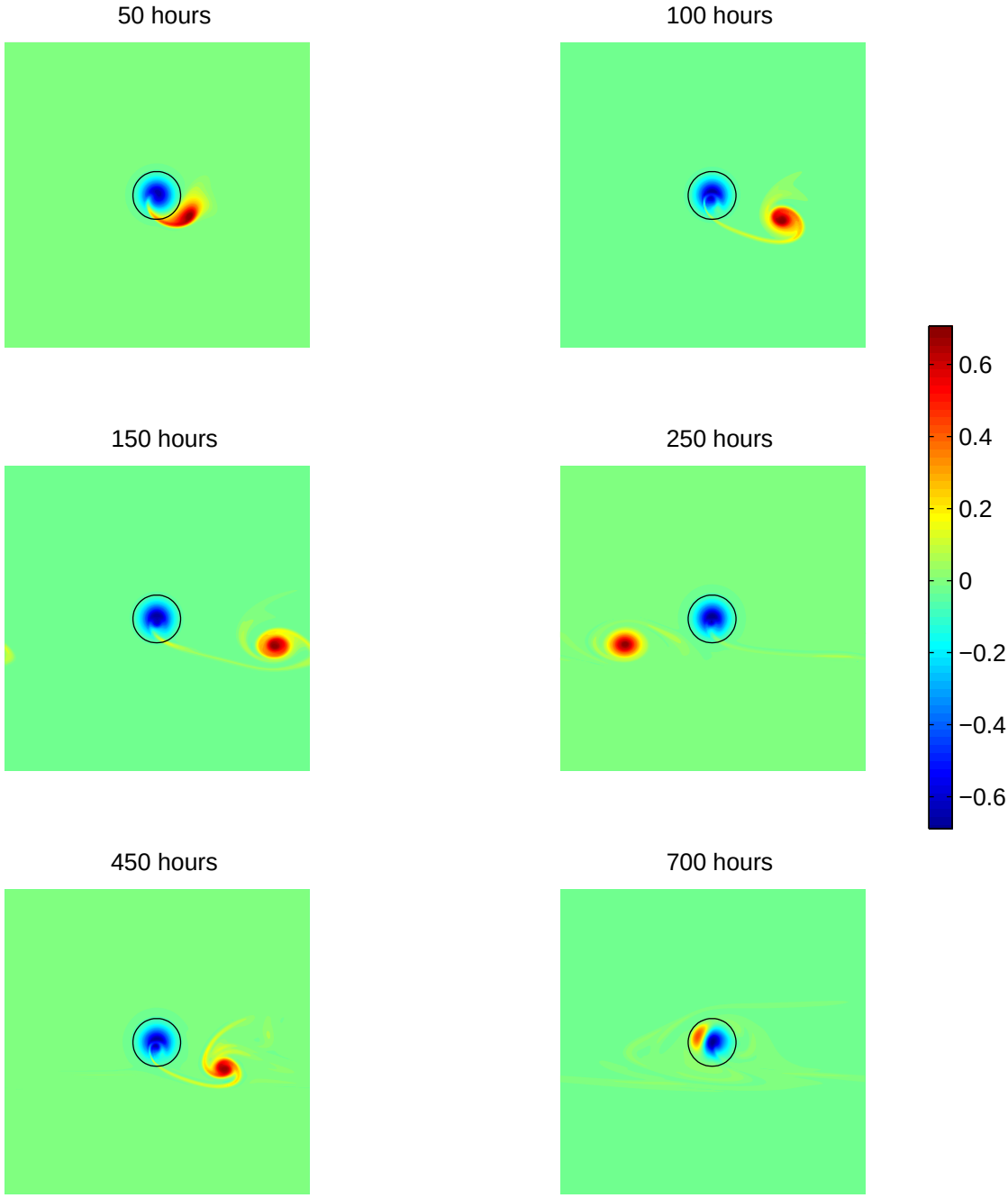

Figure 4.2: Vorticity in an initially zonal flow over 1/4 depth gaussian hill on an f-plane

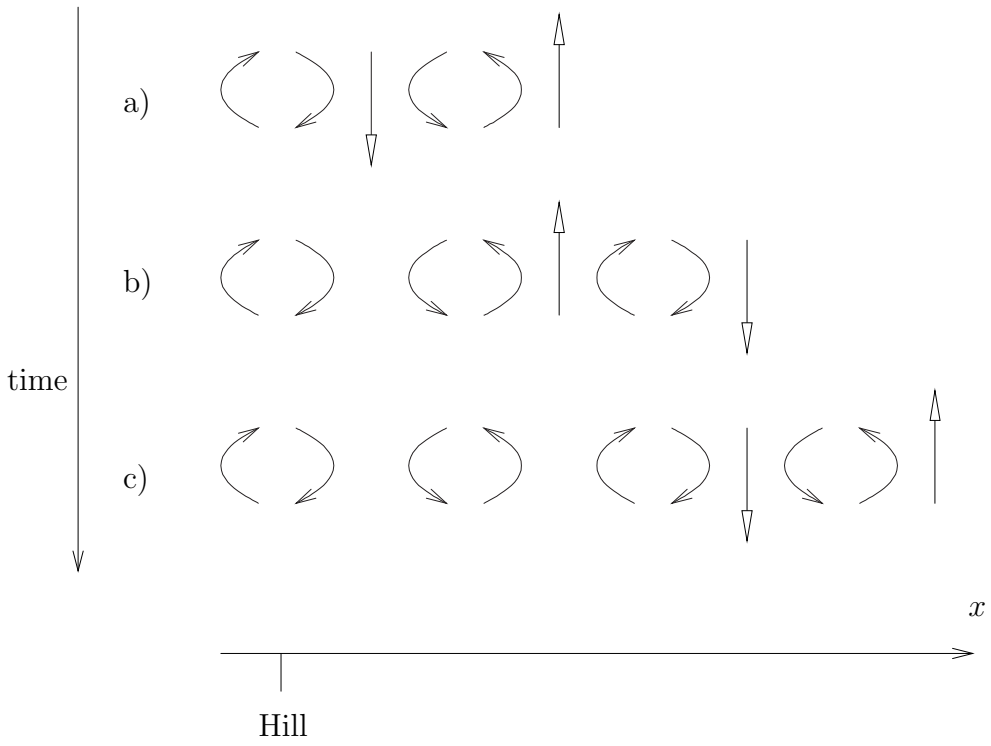

Figure 4.3: Idealised evolution of vorticity on a beta-plane over orography. For description see main text.

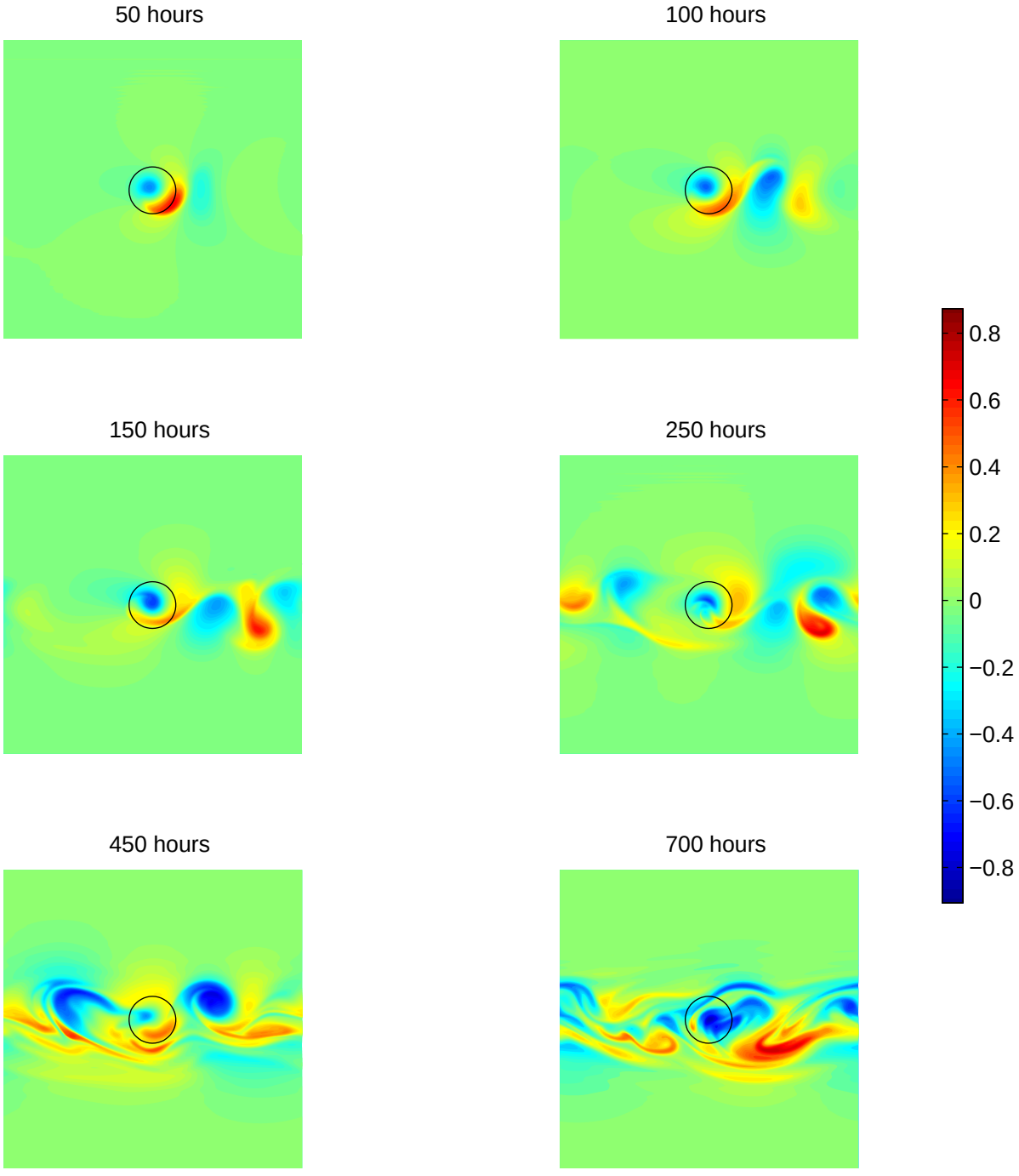

Figure 4.4: Vorticity in an initially zonal flow over 1/4 depth gaussian hill on a beta plane. β was chosen to represent a mid latitude flow.

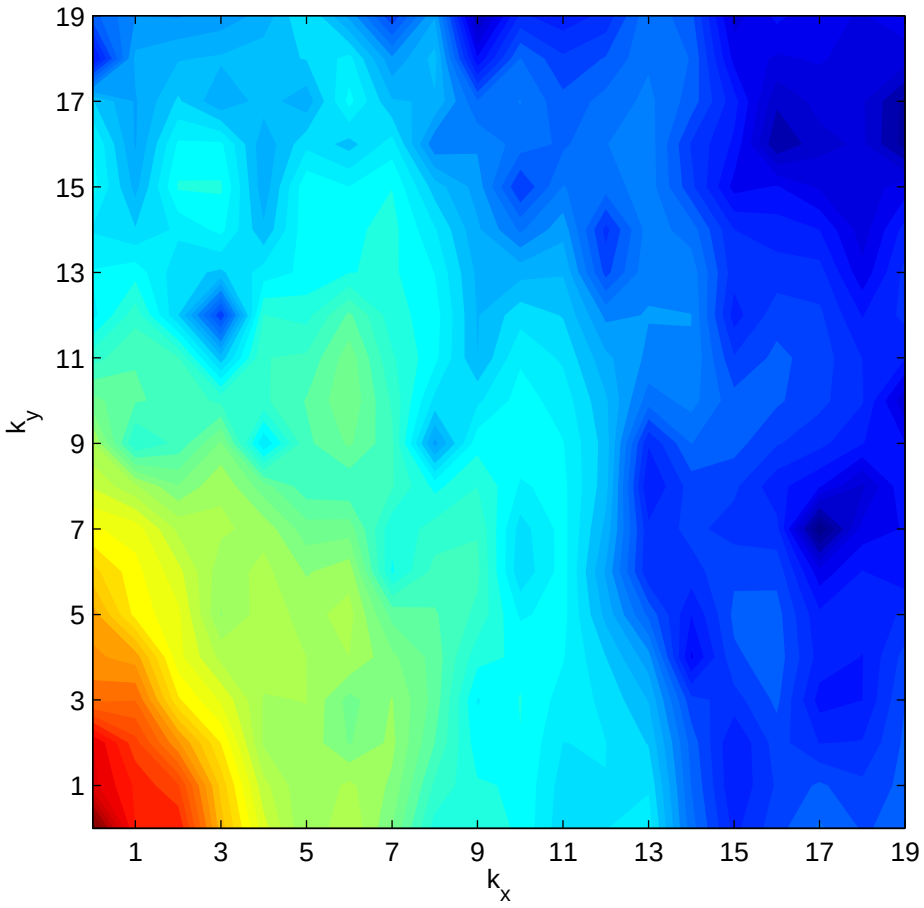

Figure 4.5: Averaged kinetic energy spectrum between 500 and 700 hours for initially zonal flow over a Gaussian hill on a beta-plane

4.2.4 Effect of orography on turbulent flow on a beta-plane

Figure 4.7 shows the evolution of vorticity on a beta plane with a hill, initialised with a thin wavenumber distribution of vorticity centred at wavenumber ten plus a zonal flow. The flow becomes dominated by Rossby waves. As with Figure 4.4 the hill appears to initiate a Rossby wave, however this is less noticible than in the zonal case.

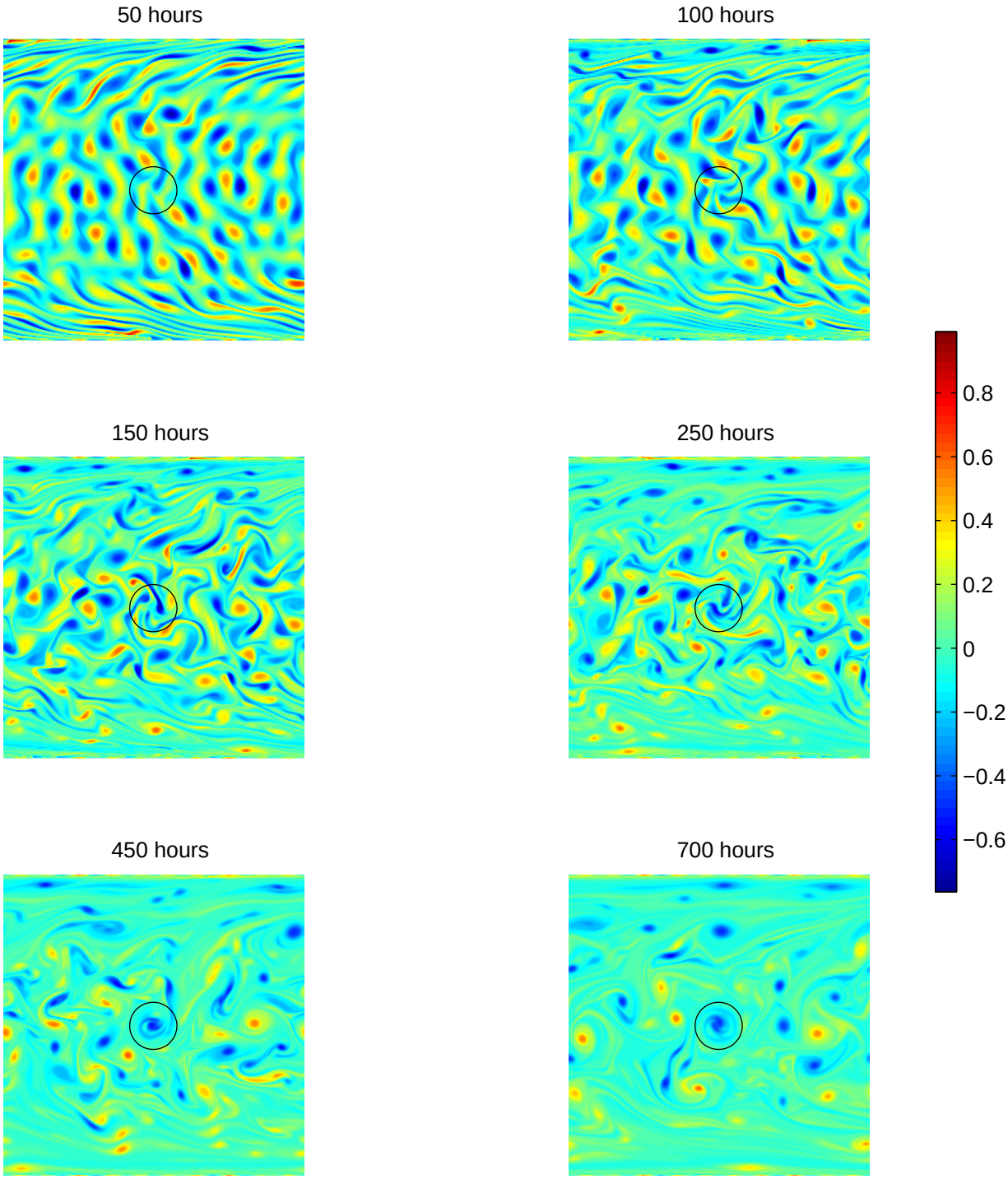

Figure 4.6: Vorticity (relative to f_0) 1/4 depth gaussian hill on an f plane. Vorticity is initialised as a thin wavenumber distribution centred around wavenumber ten. The domain is subject to a mean zonal flow.

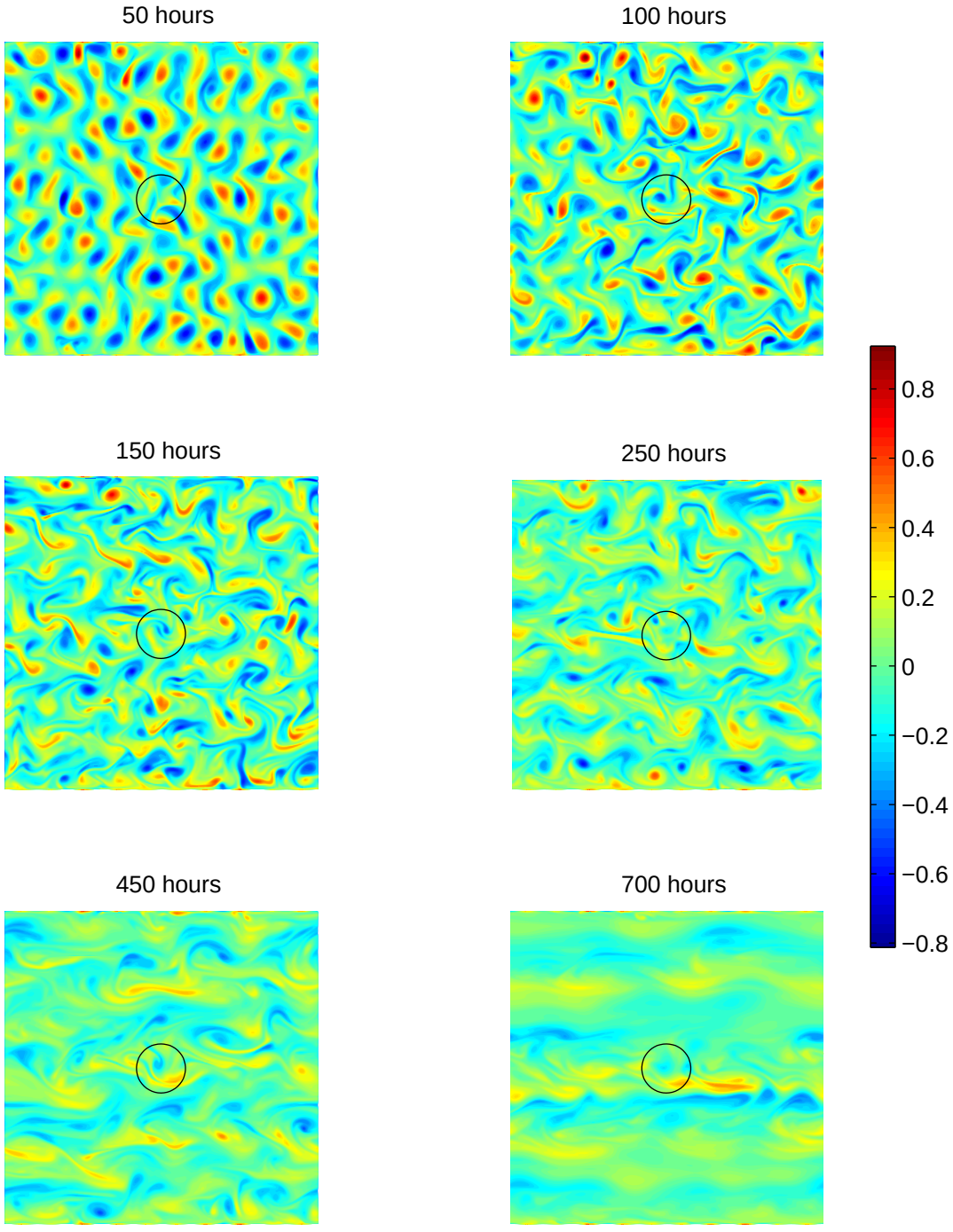

Figure 4.7: Vorticity (relative to f_0) 1/4 depth gaussian hill on a beta plane. Vorticity is initialised as a thin wavenumber distribution centred around wavenumber ten. The domain is subject to a mean zonal flow.

Chapter 5

Conclusion

We have now examined the properties of turbulent homogeneous flow in three situations; with constant rotation on a f-plane, with meridionaly varying rotation on a beta-plane and over shallow orography.

For the case of turbulent flow on an f-plane we have seen that the flow becomes approximately two dimensional and that the vorticity of fluid elements is conserved. Perhaps the most important feature is the dual cascades of energy and enstrophy. Whilst enstrophy is transfered to small scales energy is transfered to large scales; this is in contrast to the case for three dimensional flow where energy is transfered to small scales. We have seen that a flow initialised with small scale vorticity systems will evolve into a finite number of independent vortices which are advected by the base flow and rarely interact. This formation of large scale vortices has a major impact on the dynamics of the atmosphere and oceans.

We have seen that when we move from an f- to beta-plane the picture above is complicated by the formation of Rossby waves in the large scale motions, whilst the small scale motions are dominantly turbulent. The threshold wavenumber which determines whether Rossby waves or turbulence dominate is strongly dependent on β.

Finally we have investigated the effect of shallow orography on the evolution of flows. For the f-plane case we observed the formation of negative vorticity above the orography but noted that there was no significant effect on the flow downstream of the orography. The beta-plane case, however, was quite different. Again a patch of negative vorticity formed above the hill but this served to initialise a stationary Rossby wave which stretched round the domain.

As an illustration it is interesting at this stage to consider what we have seen in terms of real data. From what we have seen we expect flow in polar regions to be dominantly turbulent whilst moving towards the equator we would expect Rossby waves to become increasingly important and to occur at smaller scales. Figure 5.1 is a plot of the potential temperature at the PV=2 level (a common measure of the level of the tropopause). Higher potential temperature values indicate the tropopause is higher and implies negative vorticity whereas lower

temperatures imply that the tropopause is lower and positive vorticity.

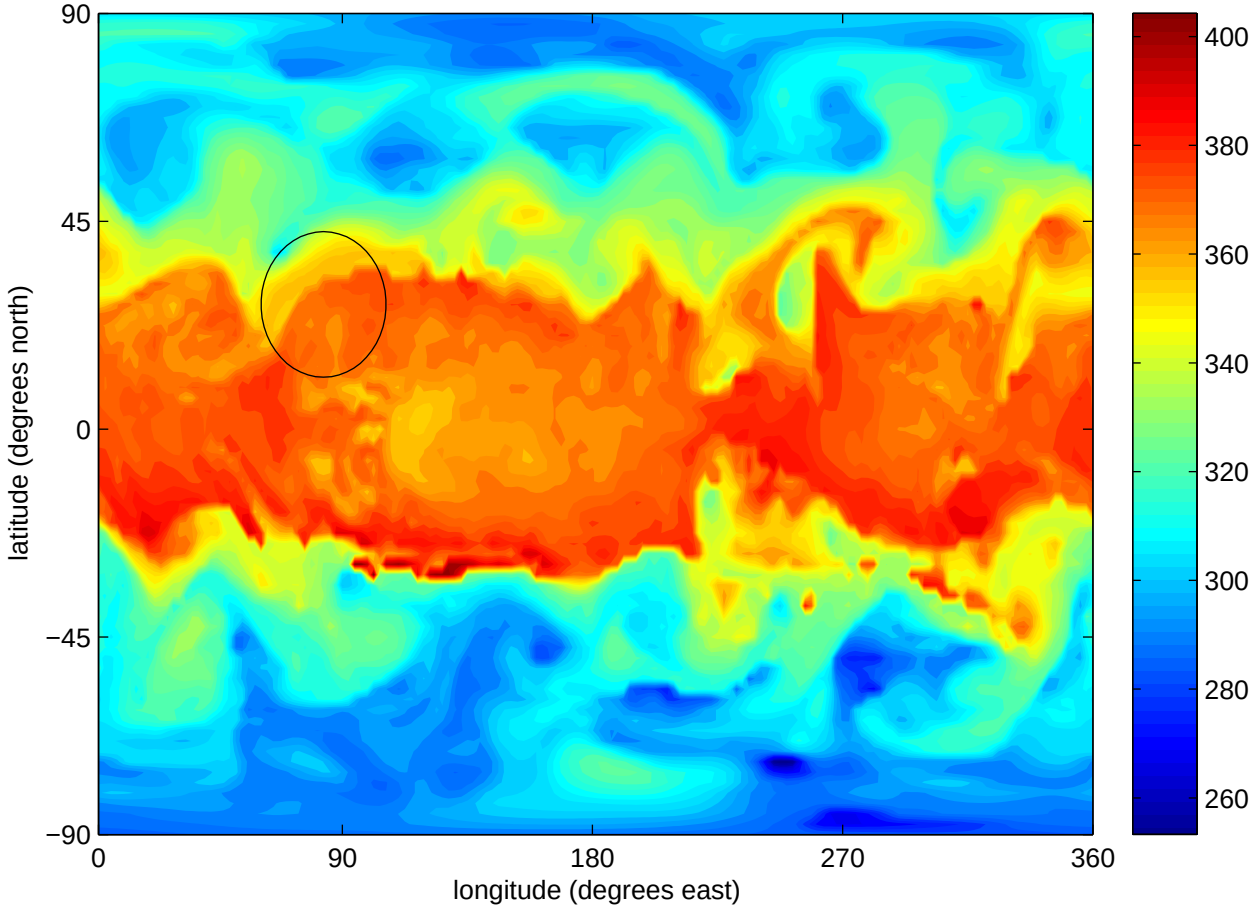

Figure 5.1: Potential temperature (K) on PV = 2PVU. 00.00 1 January 1999 UTC. Black circle indicates the approximate position of the Himalaya.

At high latitudes the flow is dominated by large wave features. These become smaller closer to the equator; this is consistent with the theory predicted in Chapter 3. There is also some evidence of turbulent eddies being formed in the mid to high latitudes. Close to the equator are what appear to be small scale turbulent eddies, these may be the result of convection. The black circle in Figure 5.1 indicates the approximate position of the Himalaya. There is some indication of Rossby wave initialisation to the West of this but it not entirely clear whether this is due to orographic forcing.

In conclusion, whilst the mechanisms described here do go some way in describing the dynamics of the atmosphere and oceans, there is much which is not described here. The most important effects result from the vertical structure of

the atmosphere and from thermal forcing and include baroclinic instability which is responsible for the generation of many mid-latitude weather systems. Nonetheless, the effects described here, in particular the formation of independent vortices and of Rossby waves provide an important starting point for understanding the dynamics of the Atmosphere and Oceans.

Appendix A

Calculation Methods

A.1 Model

The model used was adapted from Dr Maarten Ambaum's semi-Lagrangian channel model. This works by tracking the flow of fluid elements in a domain with periodic zonal boundaries and no slip meridional boundaries. The main model quantity is potential vorticity from which the vorticity and hence winds are calculated by inverting the PV field. The inversion is carried out using a spectral method in the zonal direction and by diagonalising a matrix in the meridional direction.

There are a number of advantages to a semi-Lagrangian model; the most obvious being the increase in efficiency compared to a more traditional finite difference grid point model. As the scheme is unconditionally stable it is possible to use much larger time step than would be possible with a traditional Eulerian grid point model. Another advantage is that the model's use of an advection scheme makes it easier to understand in terms of laws constructed following fluid elements.

The main disadvantage of a semi-Lagrangian model scheme is its lack of conservation for quantities which are conserved by the governing equation. In the case of these experiments this results in diffusion of the vorticity, most apparent for small time steps. To an extent this may be regarded as useful; it makes the model more realistic in that some degree of diffusion is observed an laboratory experiments. The problem is that there is no control over how much diffusion takes place and where happens, unlike an Eulerian model where it is typically added explicitly. Some work has been done to identify where these inconsistencies occur (see for example [27]) and to correct to the scheme to make it conservative but this is not included in this model.

For the results given here the model was run at 256×256 resolution, with equal grid spacing in both directions. This gives a good compromise between efficiency and level of detail in the model. A square grid was chosen as this means the model

can support the same number of wavenumbers in each direction, this is helpful when calculating the isotropic energy spectrum. The square domain comes at the expense of some realism in that the domain is intended to represent a latitude strip of the earth's atmosphere, hence the boundaries. Setting the meridional and zonal lengths of the domain to be the same compromises this somewhat. However, as the aim is really to investigate the nature of flows governed by particular differential equations rather than to reproduce any particular phenomena on in the Earth's atmosphere this is not too important.

A.2 Initialisation

A number of different methods were tried to initialise the vorticity field in the model. The first was to use a series of sin and cos functions to produce an idealised vorticity field. The problem with this method was that it tended to produce fields that were too "regular". Another method was to initialise the vorticity entirely with white noise. Whilst this produced some interesting phenomena this does not really correspond to any physical situation and concentrates all the energy and enstrophy at very high wavenumbers.

Most of the theories regarding the evolution of energy and enstrophy spectra call for a system which is initialised with a thin spectrum; this is the idea that was finally used. The vorticity is generated first in wavenumber space, using random numbers within a Gaussian envelope, centred around a specified wavenumber. This was then converted to a vorticity field by taking the inverse fast Fourier transform then using the real part. This results in an initial field which has a good mix of small scale details within a large scale structure.

A.3 Calculation of Energy and Enstrophy Spectra

Much of the analysis presented here is based on spectra of energy and enstrophy fields.

A.3.1 Energy and Enstrophy fields

The theoretical derivation of the properties of turbulence have been expressed in a finite domain with no-slip boundaries. This meant that the energy and enstrophy fields had a continuous spectrum. The model analysis, however is carries out using the fast Fourier transform. This means that the energy and enstrophy spectra will only exist at discrete wavenumbers.

Enstrophy

The enstrophy spectra is found from the vorticity field. From (2.2) vorticity may be expressed as a Fourier series. The enstrophy is then given by (2.3). Since we are only interested in the magnitude of the components we may use

$$|\hat{Z}_{\boldsymbol{k}}| = |\hat{\xi}_{\boldsymbol{k}}|^2$$

Energy

The energy components are given in terms of wind velocities u and v as

$$|\hat{E}_{\boldsymbol{k}}| = |\hat{u_{\boldsymbol{k}}}|^2 + |\hat{v_{\boldsymbol{k}}}|^2$$

where u and v are the zonal and meridional wind velocities respectively.

A.3.2 Calculation of 2D spectra

We wish to calculate the spectra making use of the fast Fourier transform (FFT), an implementation of the discrete Fourier transform. Taking the FFT of n data samples returns a Fourier space result of length n. Finding the FFT of two dimensional data is achieved by taking the FFT along each column of data in-situ, and then taking the FFT along each row.

The main problem with using the discrete Fourier transform in this situation is that it is intended for periodic data. This is not a problem for calculating the FFTs of the rows due to the periodic boundary condition, however there is a no slip boundary condition along the columns meaning that the top row is completely unrelated to the bottom row. One way round this, suggested by [18], is to pad the data with additional rows of zeros. This, however, appeared to make the problem worse in that it created an almost continuous spectrum in some places in the y direction. The other problem with adding rows is that this distorts the physical lengths corresponding to wavenumbers in the y direction when compared to the x direction, thus causing an elongation of the spectrum in the y direction. The method chosen was to linearly taper the last ten rows at each end of the data to zero. This does not entirely eliminate the problem but does suppress the noise caused by non periodicity considerably.

A.3.3 Calculation of 1D spectra

Having obtained a spectrum in two dimensional wave space it is useful to be able to obtain a one dimensional wave spectrum of E or Z with respect to wavenumber, k. The definitions for these are given for energy and enstrophy respectively by (2.5) and (2.4). The main problem is obtaining an average of the spectrum for a given wavenumber, k, given that the spectra only exist at discrete wavenumbers (because k_x, k_y are both integers).

In order to calculate the average field for a given k, the field is sampled at 50 points on a quarter circle centred at the origin with radius k. Since the field is discrete, any selected point will probably not correspond with one of the actual wavenumbers, therefor a weighted average of the four nearest wavenumbers is used to determine the field. For each k, where k is an integer, the field is averaged then multiplied by πk to give the 1D spectrum.

Bibliography

[1] D J Acheson. *Elementary Fluid Dynamics*. Oxford University Press, 1998.

[2] J G Charney. Some remaining problems in numerical weather prediction. advances in numerical weather prediction. Technical report, Traveller's Research Center, Hartford, Conn., 1966.

[3] J G Charney. Geostrophic turbulence. *Journal of the Atmospheric Sciences*, 28(6):1087–1095, 1971.

[4] J G Charney and A Eliassen. A numerical method for predicting the pertubations of the middle latitude westerlies. *Tellus*, 1:38–54, 1949.

[5] J. G. Charney, R. Fjörtoft, and J. von Neumann. Numerical integration of the barotropic vorticity equation. *Tellus*, 2(4):237–254, 1950.

[6] R E Dickinson. Rossby waves - long-period oscillations of oceans and atmospheres. *Ann. Rev. Fluid Mech.*, 1978.

[7] J R Holton. *An Introduction to Dynamic Meteorology*. Academic Press, 1992.

[8] J R Holton. The second harwitz memorial lecture: Stationary planetary waves. *Bulletin of the American Metorological Society*, 74(9):1735–1742, September 1993.

[9] I N James. *Introduction to Circulating Atmospheres*. Cambridge University Press, 1994.

[10] A. N. Kolmogorov. The local structure of turbulence in incompressible fluid at very high reynolds number. *Dokl. Acad. Sci. USSR.*, 30:299–303, 1941.

[11] R H Kraichnan. Inertial ranges in two dimensional turbulence. *The Physics of Fluids*, 10(7):1417–1423, July 1967.

[12] D K Lilly. Numerical simulation of two-dimensional turbulence. *Physics of Fluids Supplement II*, pages 240–249, 1969.

[13] M E Maltrud and G K Vallis. Energy spectra and coherent structures in forced two-dimensional and beta-plane turbulence. *Journal of Fluid Mechanics*, 228:321–342, 1991.

[14] J C McWilliams. Statistical properties of decaying geostrophic turbulence. *Journal of Fluid Mechanics*, 198:199–230, 1989.

[15] J C McWilliams. The vortices of geostrophic turbulence. *Journal of Fluid Mechanics*, 219:387–404, 1990.

[16] J C McWilliams. The vortices of two dimensinal turbulence. *Journal of Fluid Mechanics*, 219:361–385, 1990.

[17] J C McWilliams. The emergence of isolated coherent vortices in turbulent flow. *Journal of Fluid Mechanics*, 146:21–43, 1994.

[18] W H Press, S A Teukolsky, W T Vetterling, and B P Flannery. *Numerical Recipies in Fortran*. Cambridge University Press, 1992.

[19] P B Rhines. Waves and turbulence on a beta-plane. *J. Fluid Mech.*, 69(3):417–443, 1975.

[20] P B Rhines. Geostrophic turbulence. *Ann. Rev. Fluid Mech.*, 11:401–441, 1979.

[21] Lewis F. Richardson. *Weather Predictions by Numerical Process*. Cambridge University Press, 1922.

[22] C G Rossby. On the propagation of frequencies and energy in certain types of oceanic and atmospheric waves. *Journal of Meteorology*, 2:187–204, 187-204.

[23] C G Rossby. Relation between variations in the intensity of the zonal circulation of the atmosphere and the displacements of the semi-permenant centres of action. *Journal of Marine Research*, 2:38–55, 1939.

[24] C G Rossby. Planetary flow patterns in the atmosphere. *Quarterly Journal of the Royal Meteorological Society*, 66:68–87, 1945.

[25] G K Vallis. *Lecture Notes in Geostrophic Turbulence*. Princeton University, 1999.

[26] G K Vallis and M E Maltrud. Generation of mean flows and jets on a beta plane and over topography. *Journal of Physical Oceanography*, 23(7):1346–1362, July 1993.

[27] M Zerroukat, N Wood, and A Staniforth. Slice: A semi-lagrangian inherently conserving and efficient scheme for transport problems. *Quarterly Journal of the Royal Meteorological Society*, 128, 2002.